

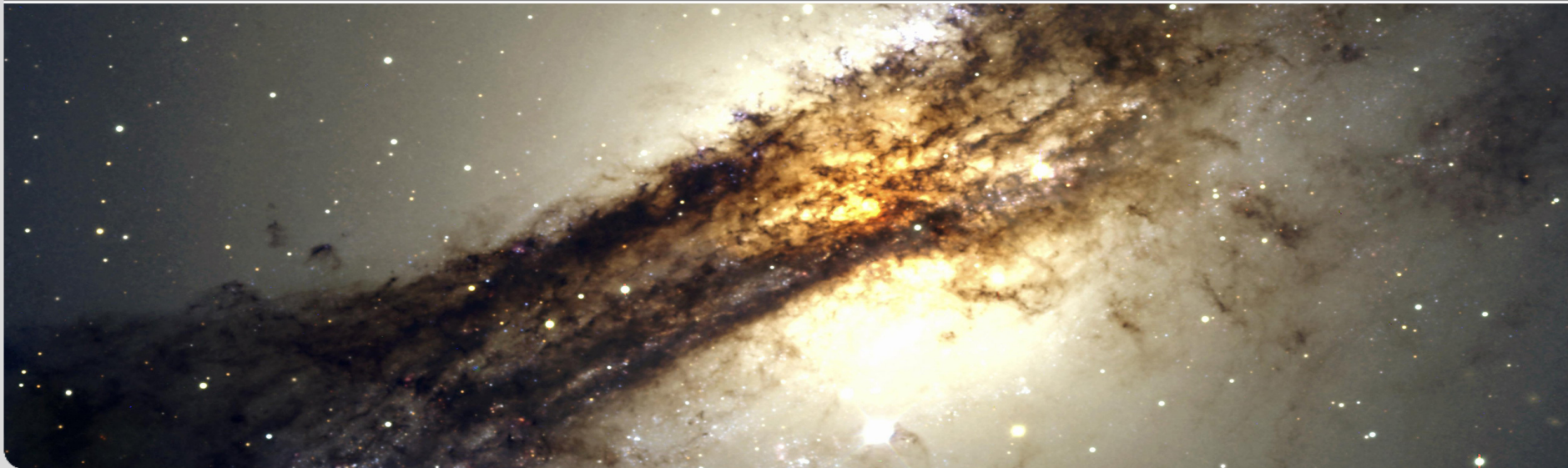
The Pierre Auger Observatory: upgrade and prospects in the EeV region.

A. M. Botti^{1,2}

Research Technique Seminar 09/10/2019

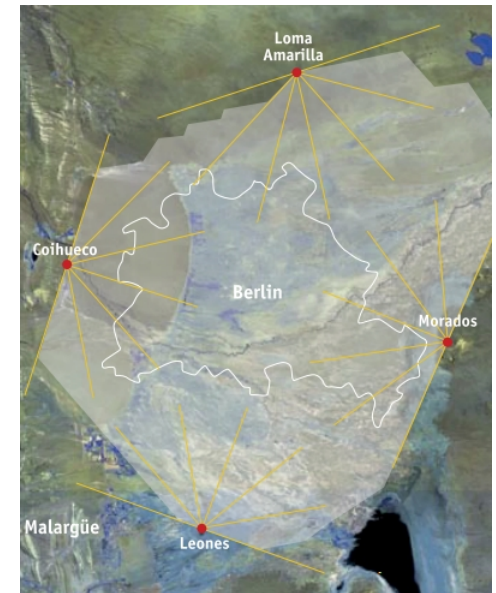
¹ Instituto de Tecnologías en Detección y Astropartículas, CNEA-CONICET-UNSAM

² Institute of Nuclear Physics (IKP), Karlsruhe Institute of Technology (KIT)

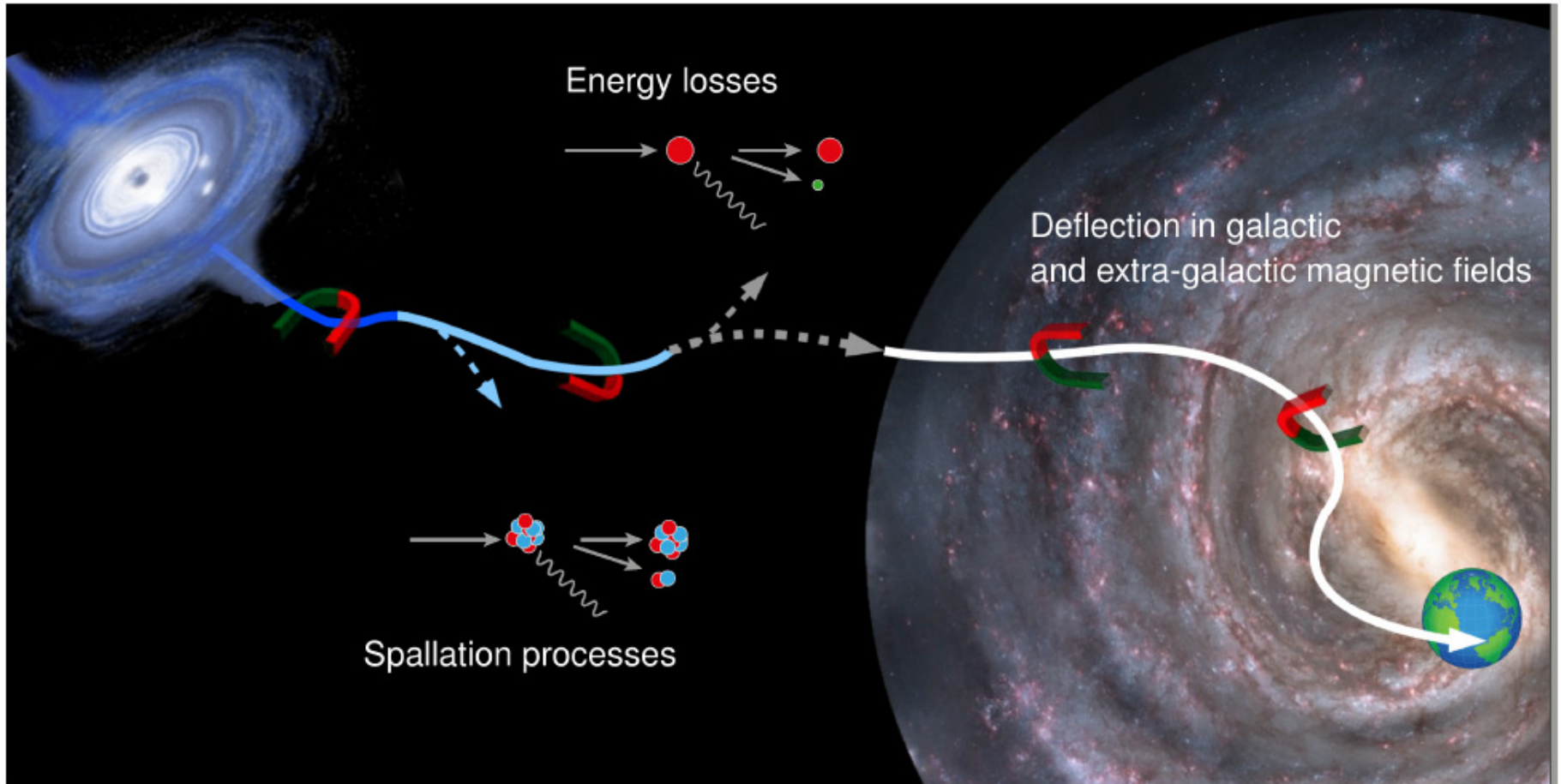


Outline

- **Introduction:**
 - Ultra High Energy Cosmic Rays.
 - Extensive Air Showers.
- **The Pierre Auger Observatory:**
 - Detectors.
 - Summary of physical results.
- **AugerPrime.**
- **Underground Muon Detector:**
 - Silicon photomultipliers.
 - Noise sources.
 - Calibration and performance.

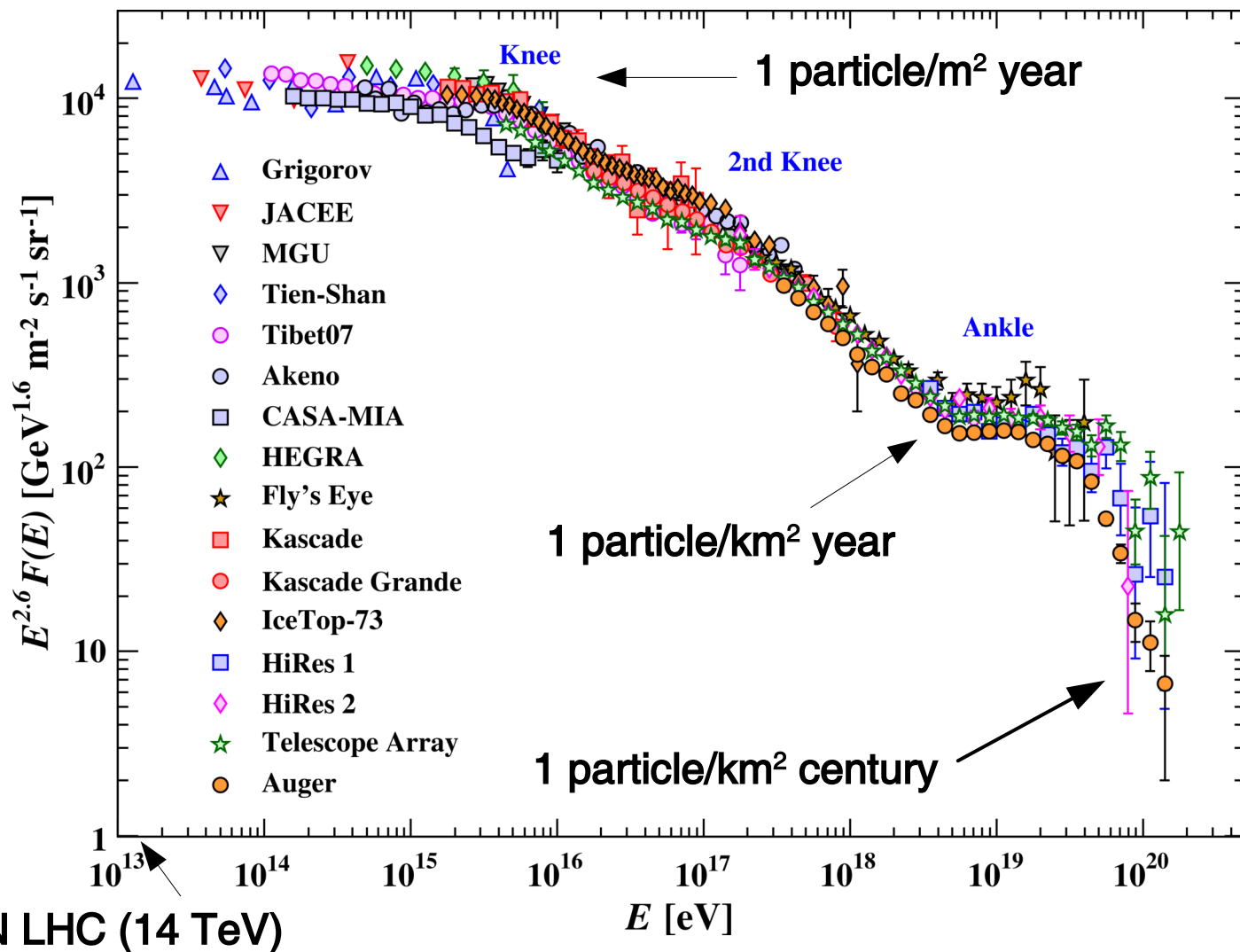
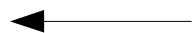


Ultra High Energy Cosmic Rays



(Ultra High Energy) Cosmic Rays

1 particle/m² sec

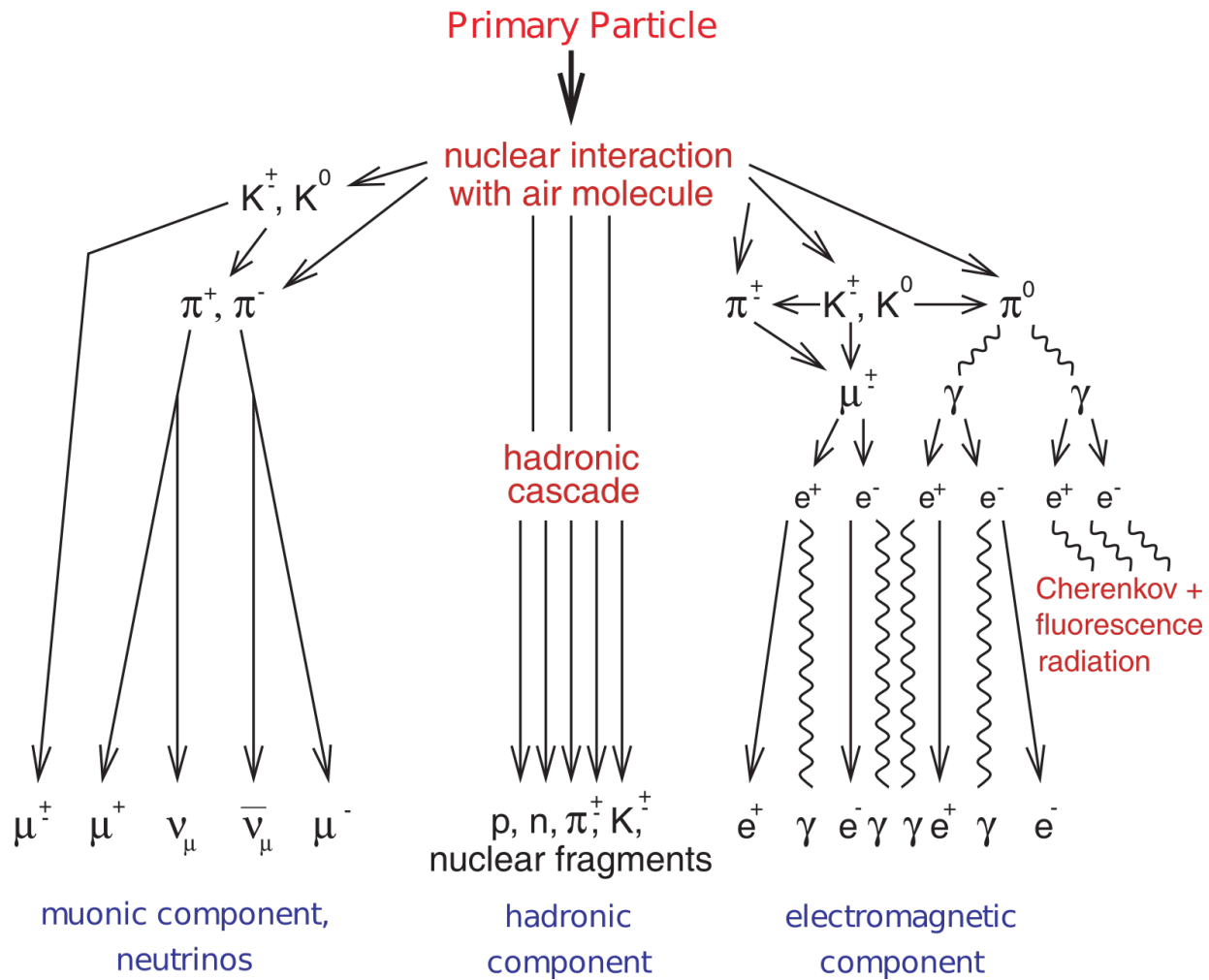


FNAL
Tevatron
(2 TeV)

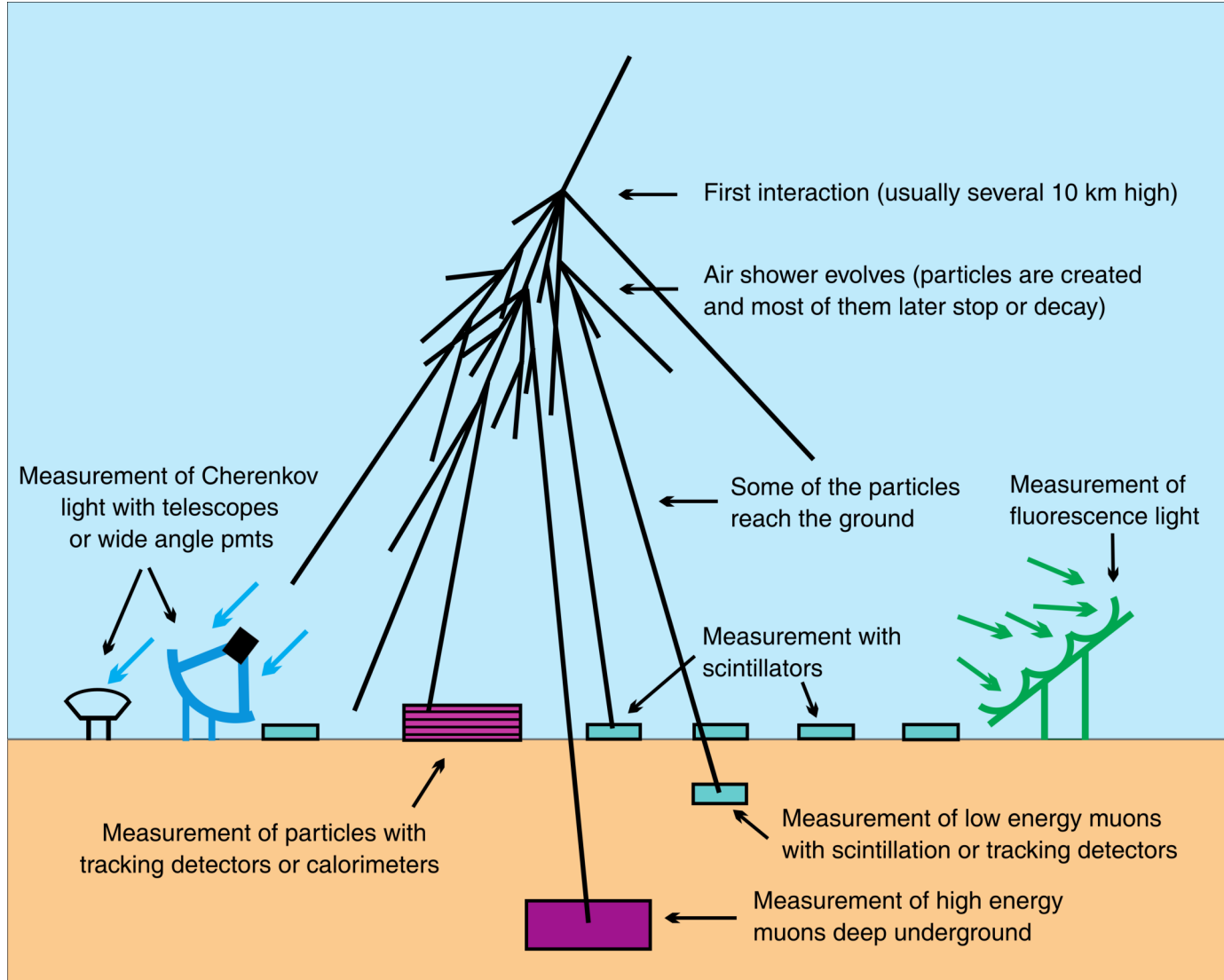


CERN LHC (14 TeV)

Extensive air showers



Extensive air showers

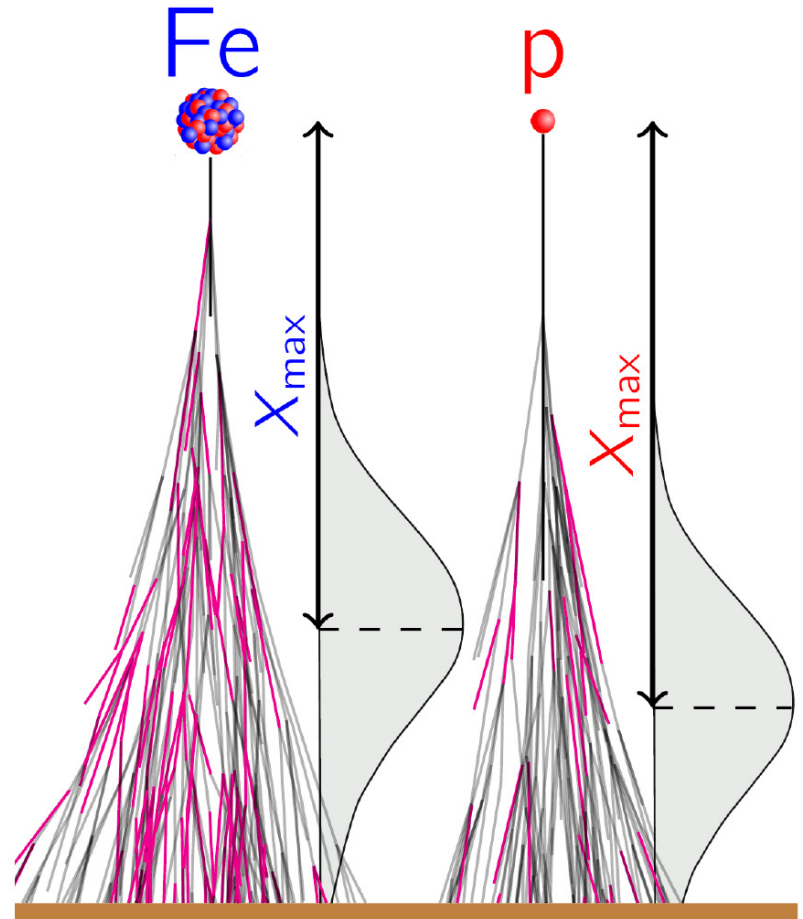


Extensive air showers

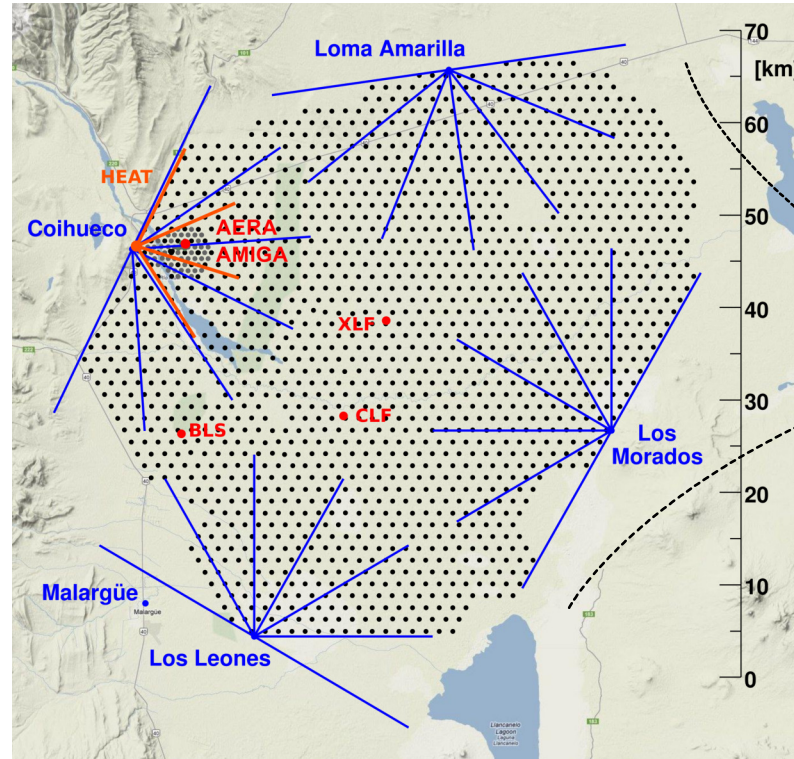
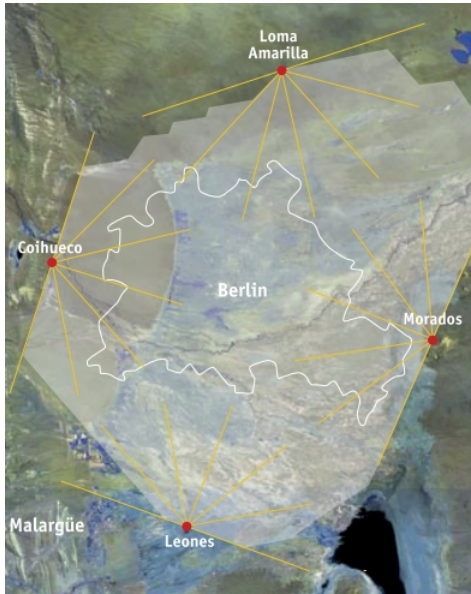
Depth of **EAS** Maximum development (X_{\max}) \rightarrow
Mass composition
and **energy**

Muon content \rightarrow **Mass**
composition and **energy**

Electromagnetic
content \rightarrow **Energy**



The Pierre Auger Observatory



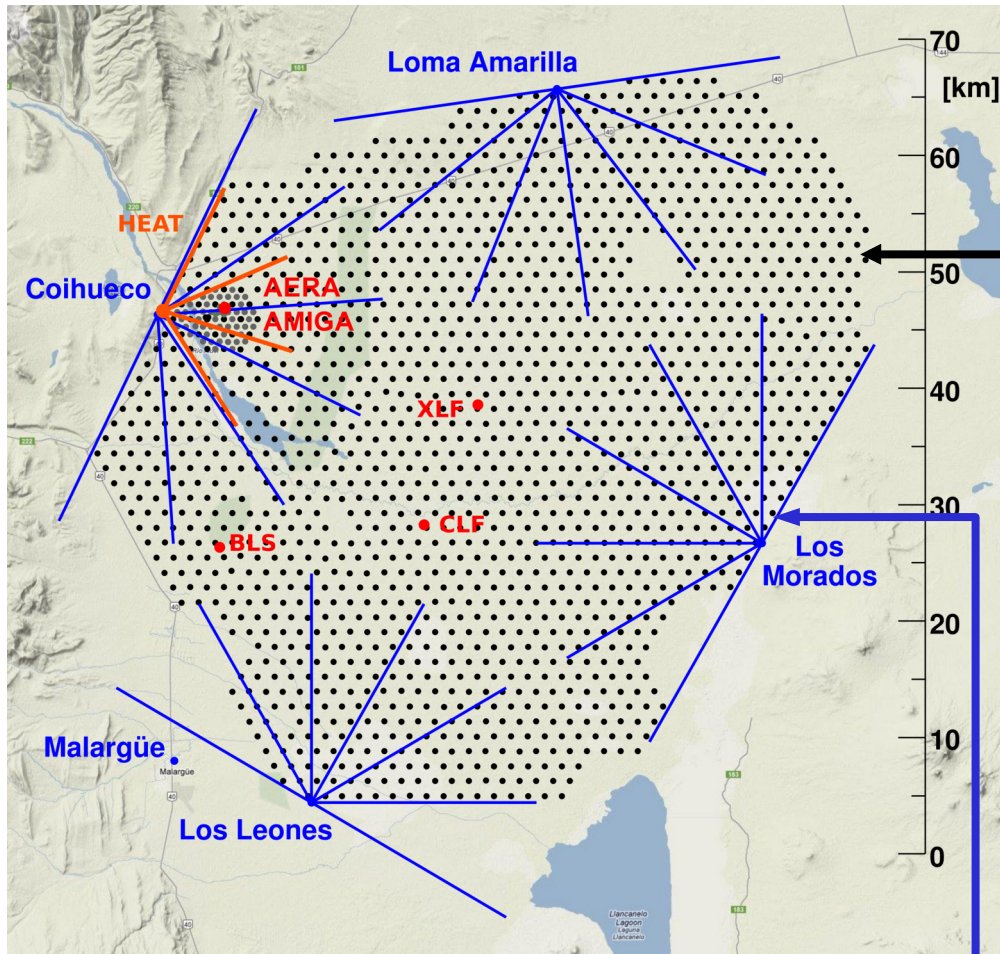
Berlin ~ 890 km²

Surface Detector ~ 3000 km²

Buenos Aires City ~ 203 km²

Chicago ~ 606 km²

The Pierre Auger Observatory



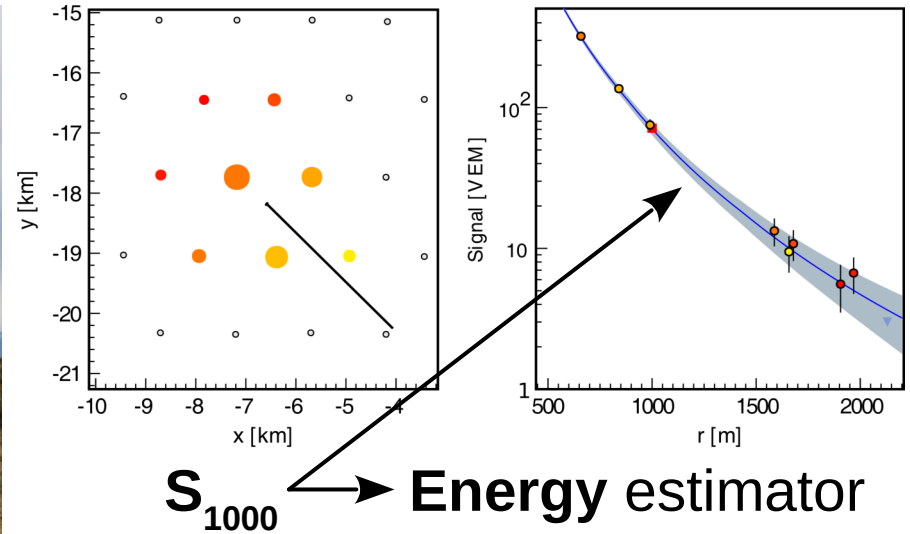
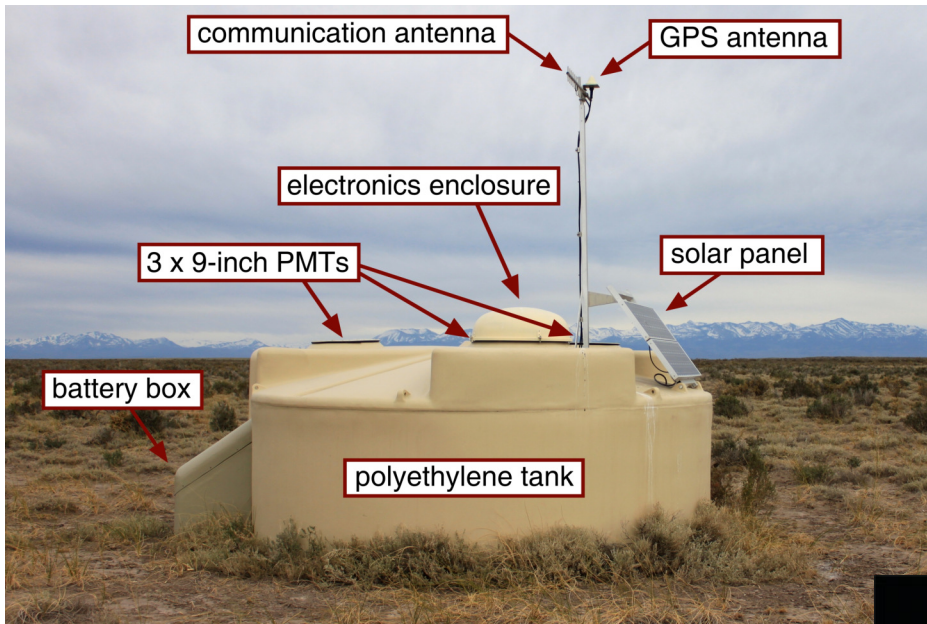
SD

- 3000 km² array
- 1660 WCD
- 3.6 m x 1.2 m
- 1.5 km between WCD

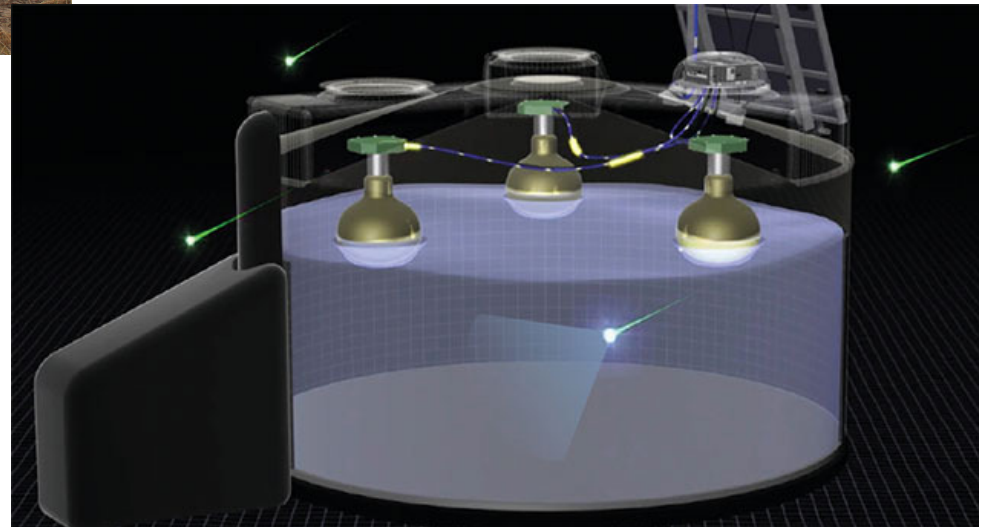
FD

- 27 fluorescence telescopes
- 4 buildings

Surface Detector (1660 WCD)



3.6 m diameter
1.2 m height
12000 l water
3x 9-in diameter **PMTs**
530 kg

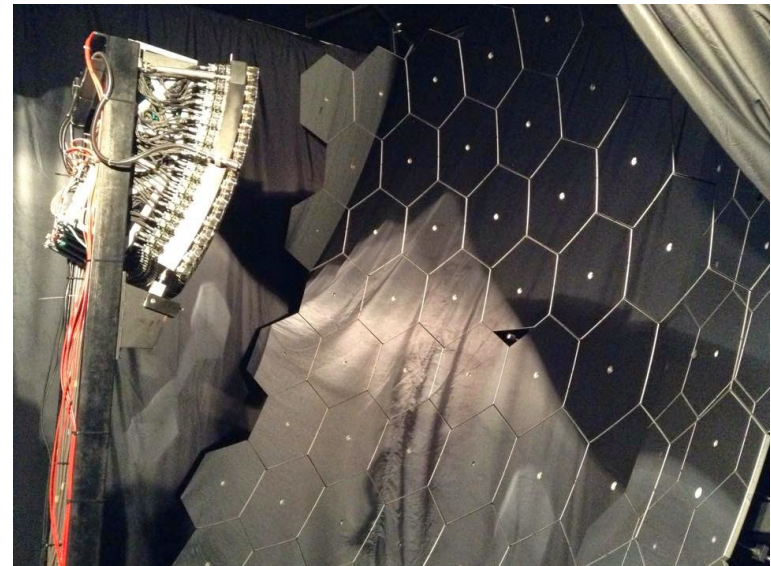
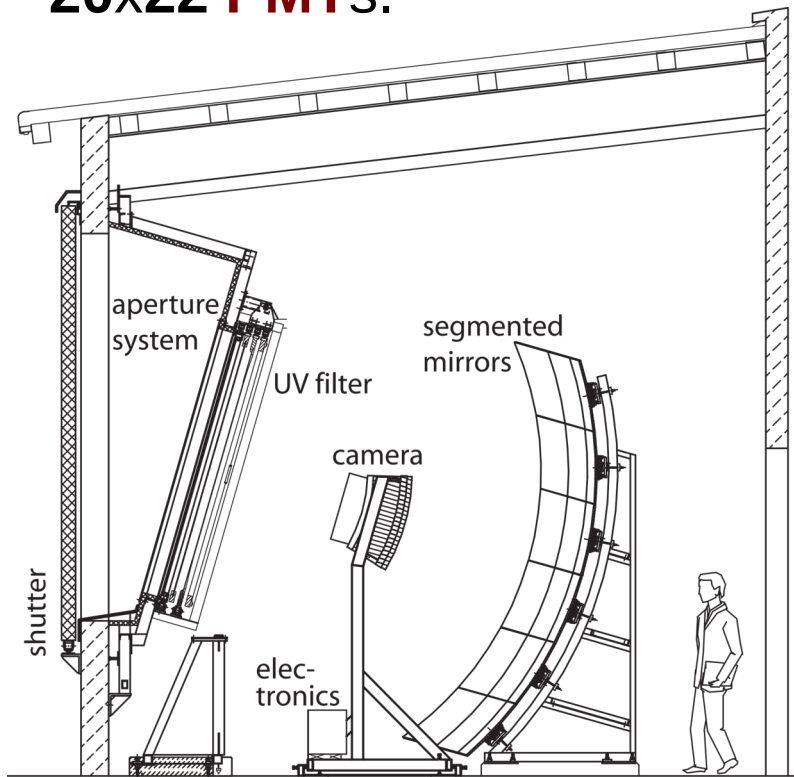


Fluorescence Detector

30° x 30° field of view.

Each building 180°.

20x22 **PMTs**.

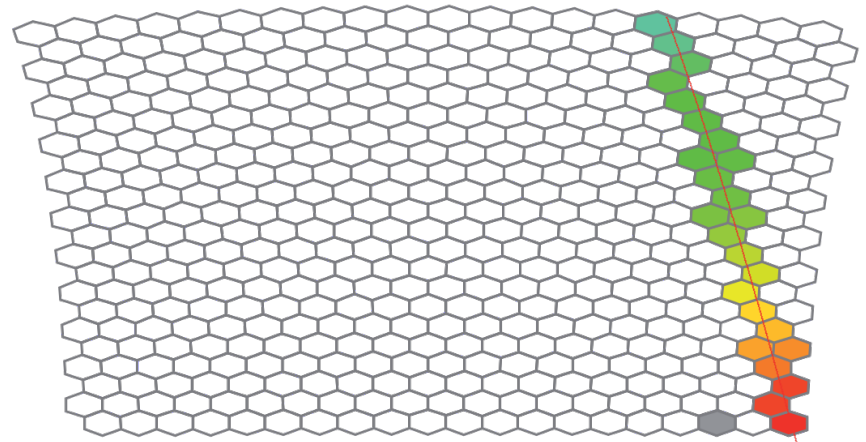
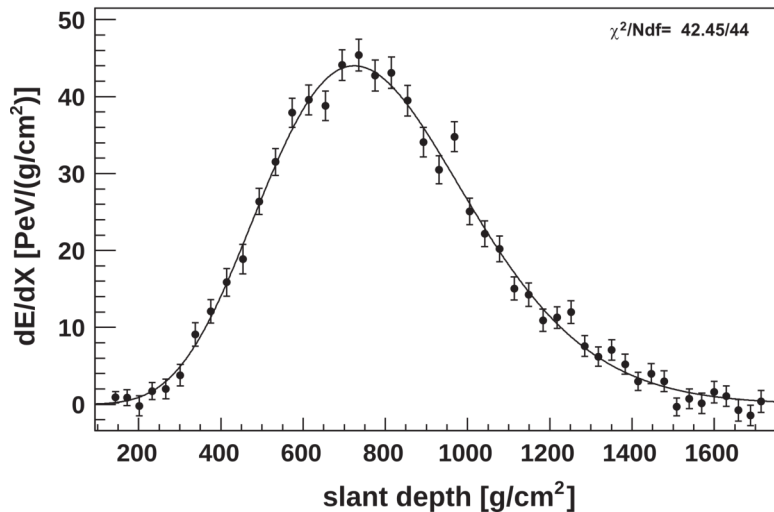
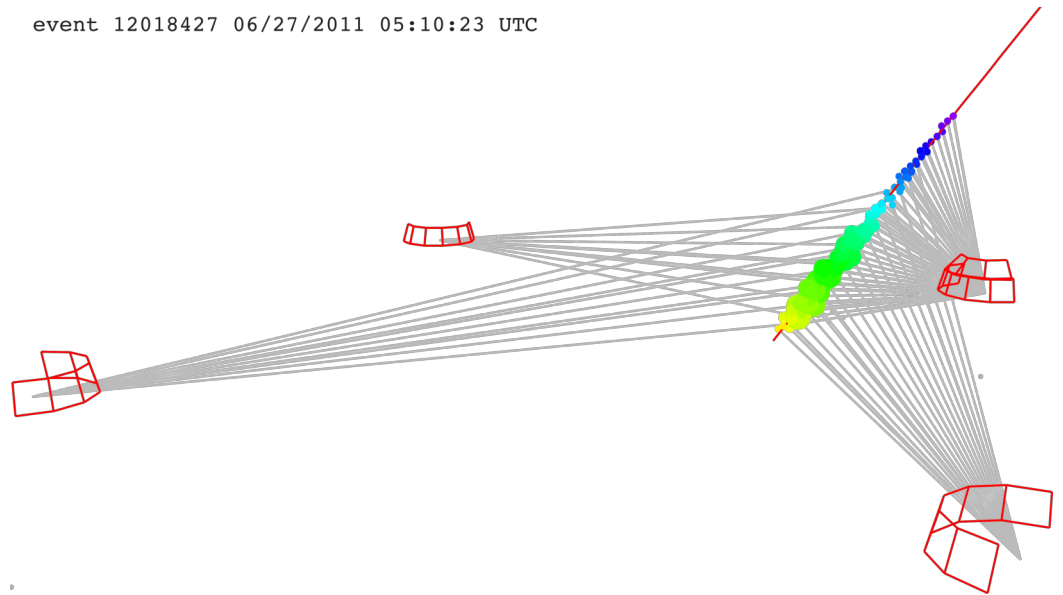


Fluorescence Detector

event 12018427 06/27/2011 05:10:23 UTC

Calorimetric energy.

X_{\max} → Energy and composition.



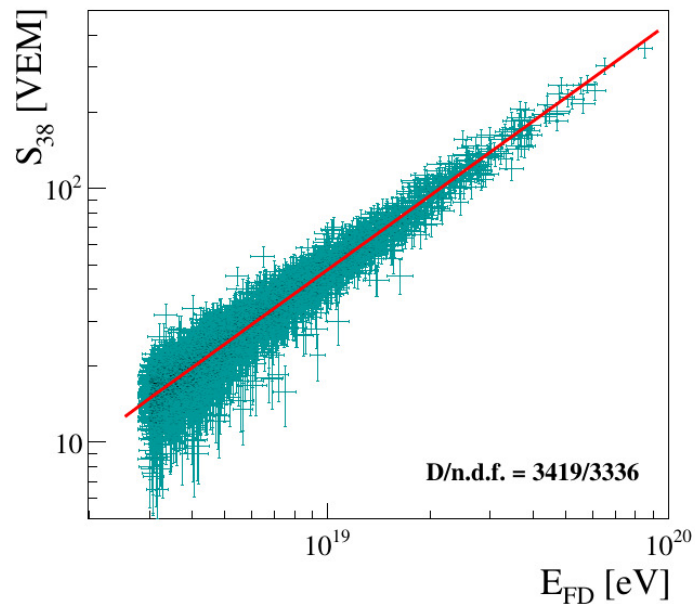
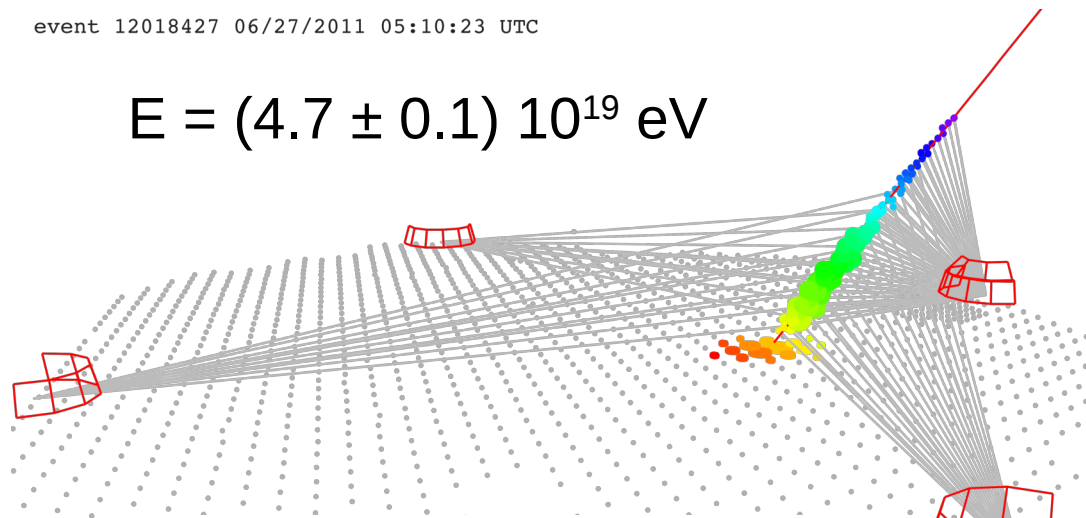
Hybrid detection

event 12018427 06/27/2011 05:10:23 UTC

$$E = (4.7 \pm 0.1) 10^{19} \text{ eV}$$

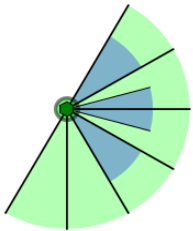
Combine detectors to reduce **systematics**.

Cross calibrate.

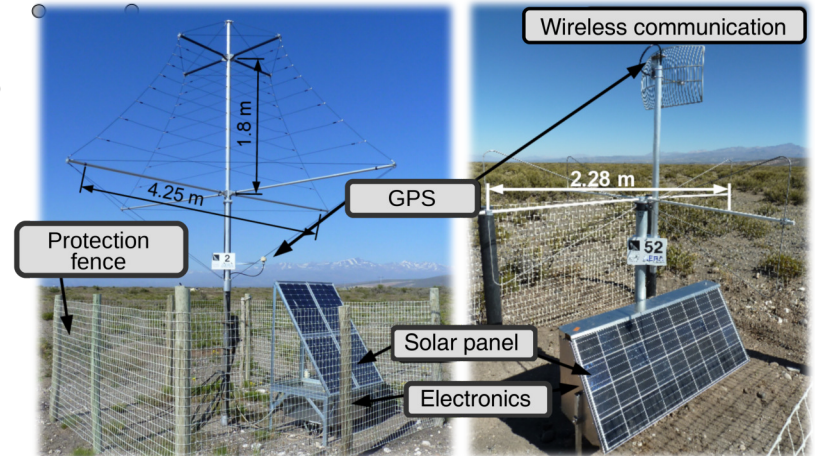
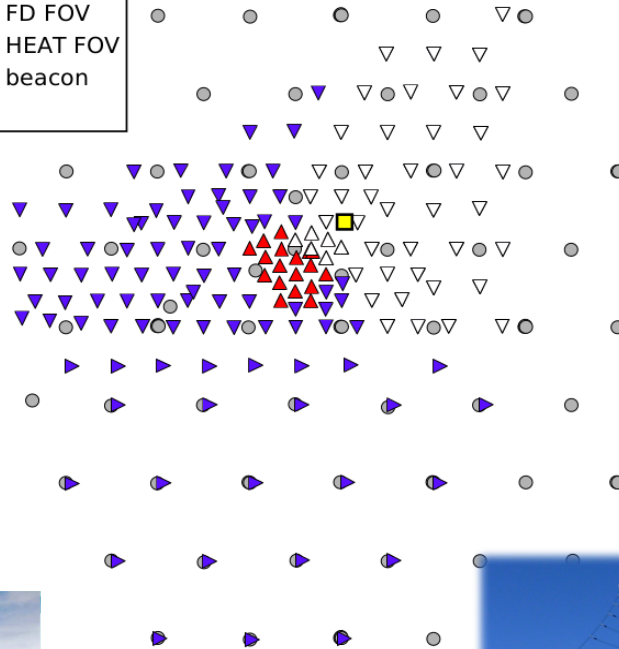


Low energy enhancements

- | | |
|---------------------------------|------------|
| ▲ AERA24 LPDA, ext. trig. | ■ CRS |
| △ AERA24 LPDA, int. trig. | ● FD site |
| ▽ AERA124 butterfly, int. trig. | ■ FD FOV |
| ▼ AERA124 butterfly, ext. trig. | ■ HEAT FOV |
| ▶ AERA153 butterfly, ext. trig. | ● beacon |
| ● SD station | |



1 km



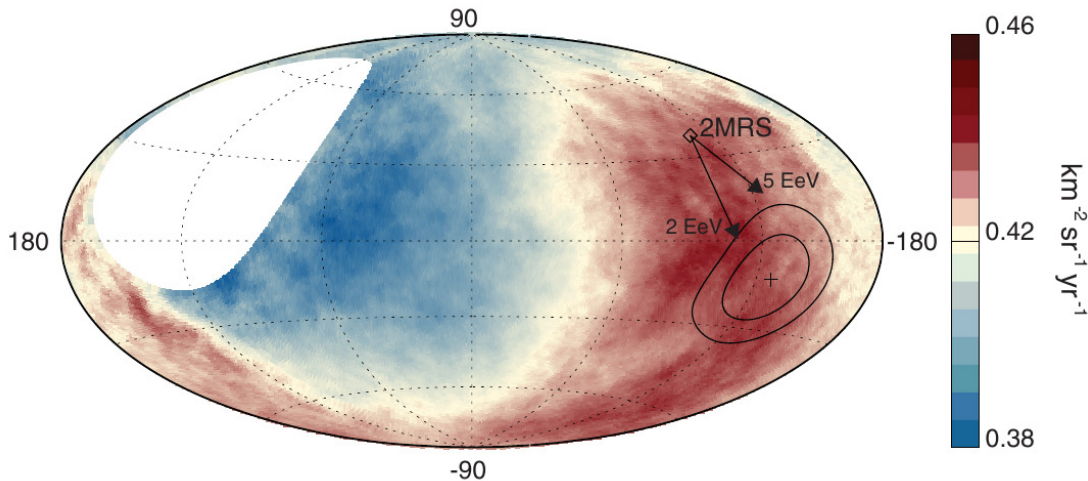
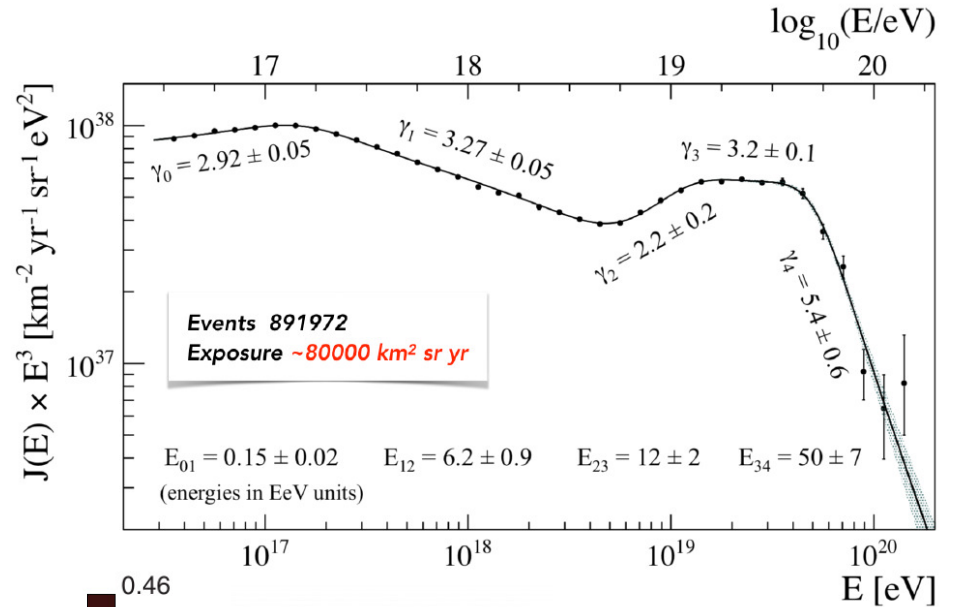
Results

Spectrum:

Flux suppression confirmed.

2nd knee was observed.

Highest statistics at UHE.



Anisotropy:

Dipole away from galactic center \longrightarrow
Strong evidence of extragalactic origin
@ $E > 8 \cdot 10^{18}$ ev.

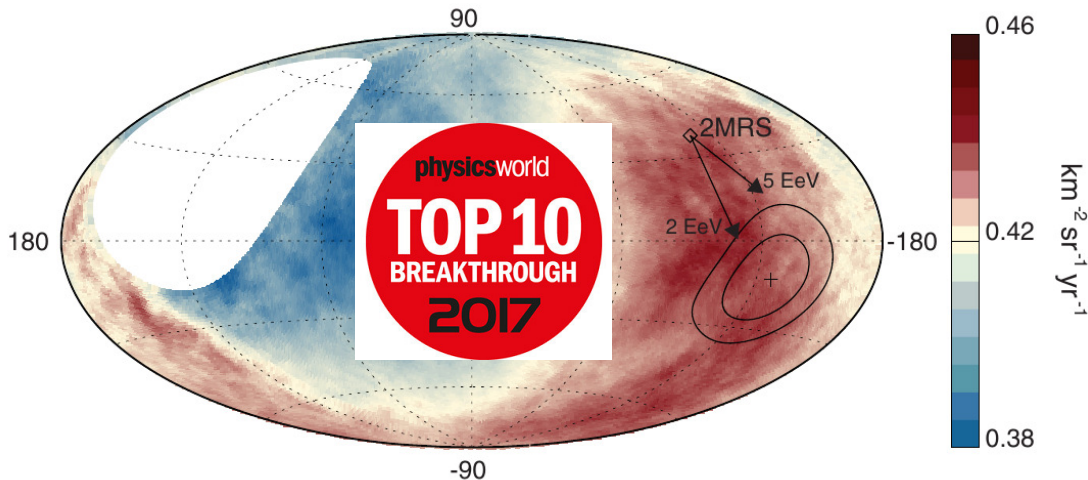
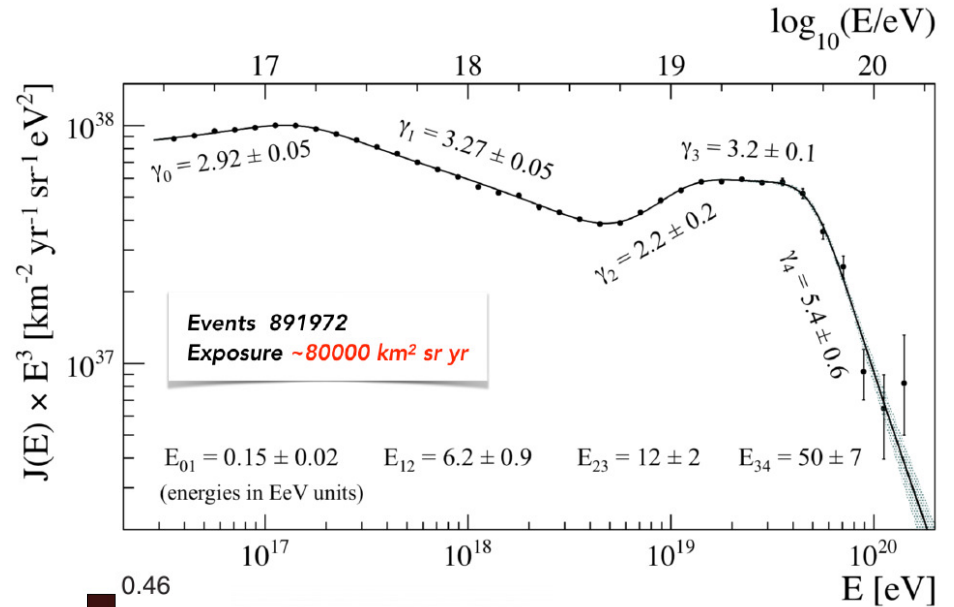
Results

Spectrum:

Flux suppression confirmed.

2nd knee was observed.

Highest statistics at UHE.



Anisotropy:

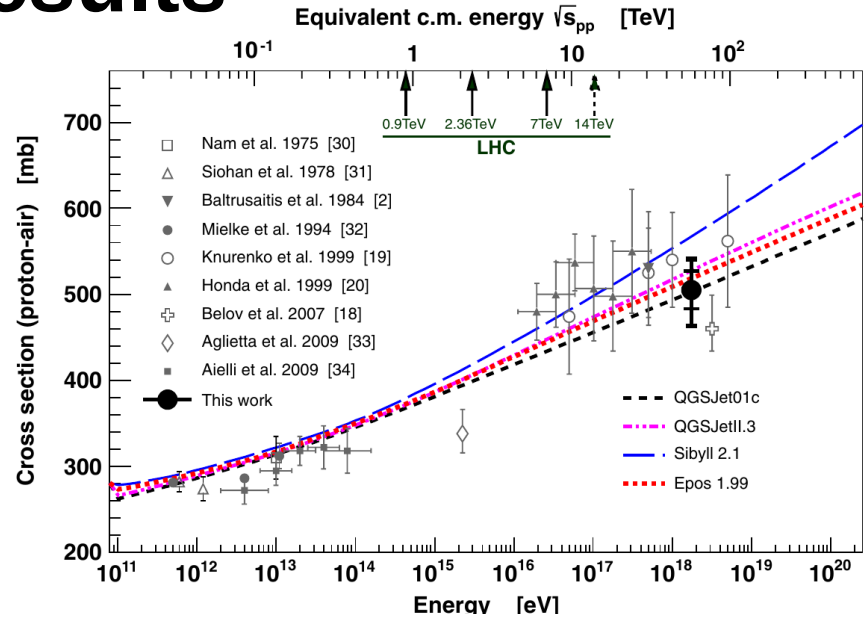
The Pierre Auger Collaboration, Science 357, 1266–1270 (2017)

"To the Pierre Auger Observatory collaboration for showing that ultra-high-energy cosmic rays come from outside the Milky Way."

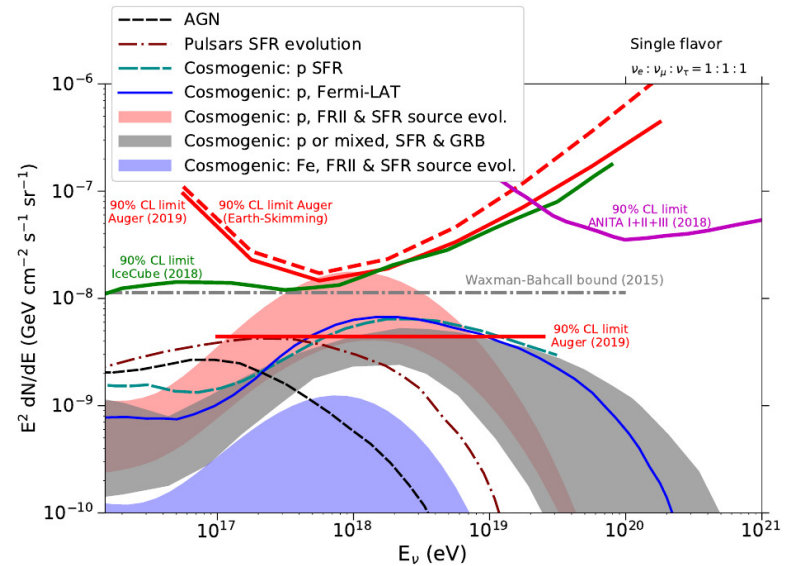
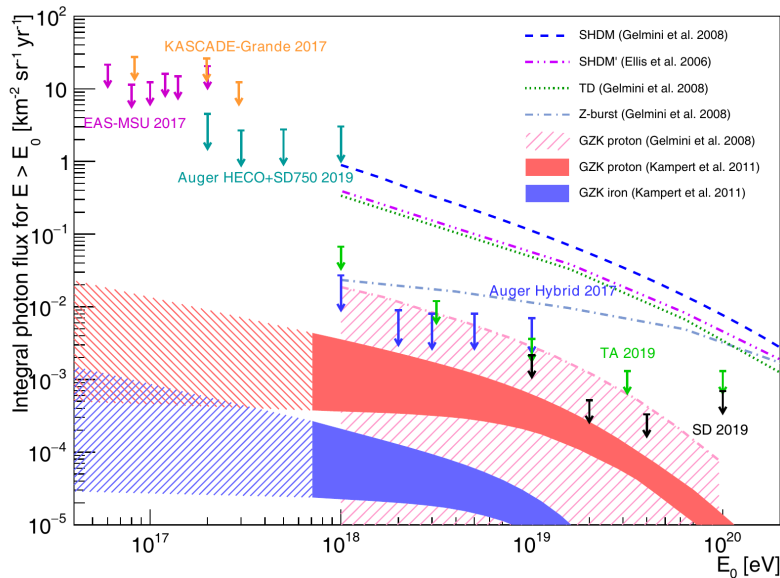
Results

Cross section proton-air (and proton-proton):

Study hadronic models at energies above LHC
($57 \pm 0.3 \pm 6$) TeV



Photon and neutrino flux:



Results

Multi-messenger Observations of a Binary Neutron Star Merger

LIGO Scientific Collaboration and Virgo Collaboration, Fermi GBM, INTEGRAL, IceCube Collaboration, AstroSat Cadmium Zinc Telluride Imager Team, IPN Collaboration, The Insight-Hxmt Collaboration, ANTARES Collaboration, The Swift Collaboration, AGILE Team, The 1M2H Team, The Dark Energy Camera GW-EM Collaboration and the DES Collaboration, The DLT40 Collaboration, GRAWITA: GRAvitational Wave Inaf TeAm, The Fermi Large Area Telescope Collaboration, ATCA: Australia Telescope Compact Array, ASKAP: Australian SKA Pathfinder, Las Cumbres Observatory Group, OzGrav, DWF (Deeper, Wider, Faster Program), AST3, and CAASTRO Collaborations, The VINROUGE Collaboration, MASTER Collaboration, J-GEM, GROWTH, JAGWAR, Caltech-NRAO, TTU-NRAO, and NuSTAR Collaborations, Pan-STARRS, The MAXI Team, TZAC Consortium, KU Collaboration, Nordic Optical Telescope, ePESSTO, GROND, Texas Tech University, SALT Group, TOROS: Transient Robotic Observatory of the South Collaboration, The BOOTES Collaboration, MWA: Murchison Widefield Array, The CALET Collaboration, IKI-GW Follow-up Collaboration, H.E.S.S. Collaboration, LOFAR Collaboration, LWA: Long Wavelength Array, HAWC Collaboration, **The Pierre Auger Collaboration**, ALMA Collaboration, Euro VLBI Team, Pi of the Sky Collaboration, The Chandra Team at McGill University, DFN: Desert Fireball Network, ATLAS, High Time Resolution Universe Survey, RIMAS and RATIR, and SKA South Africa/MeerKAT (See the end matter for the full list of authors.)

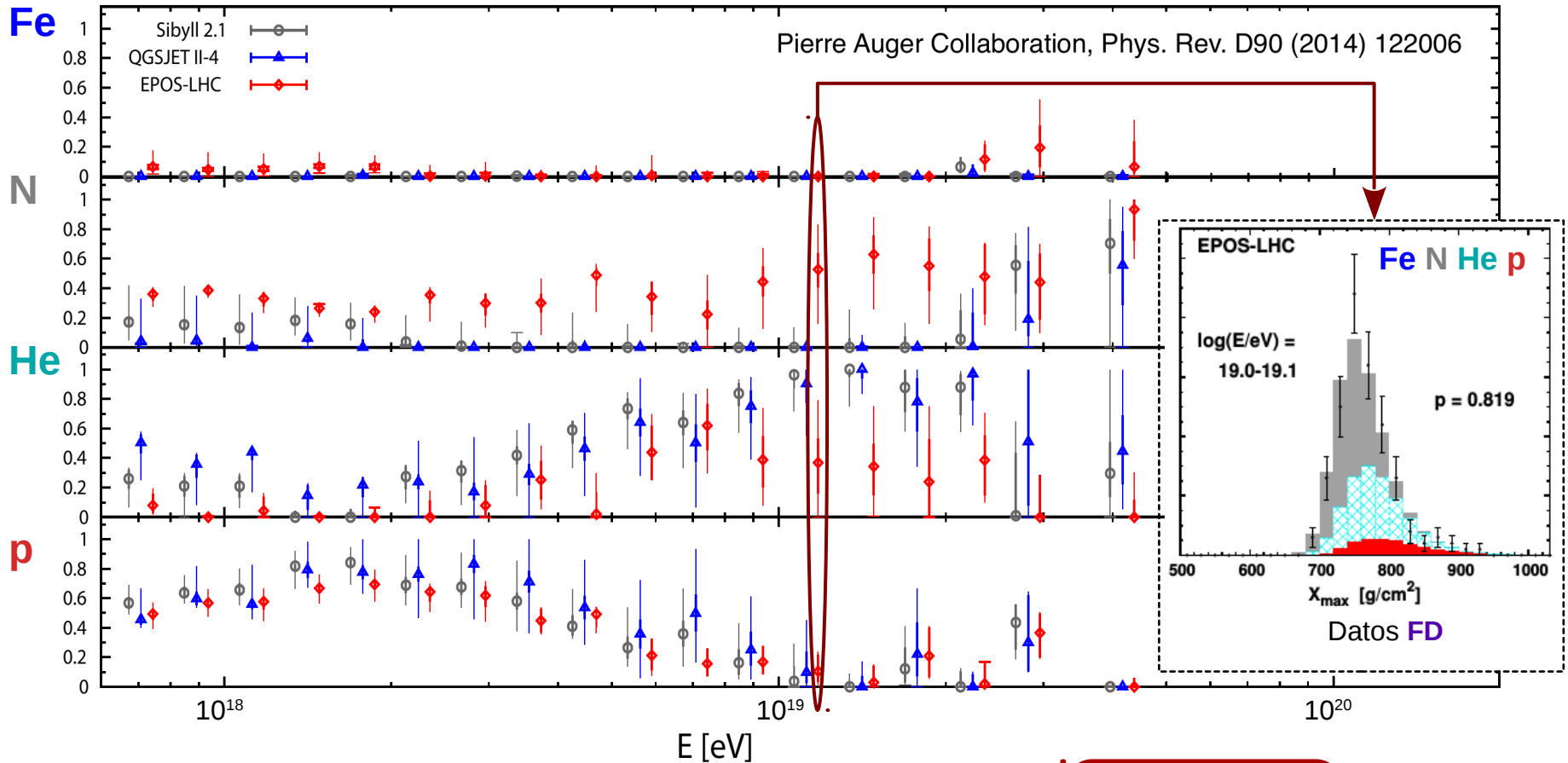
Received 2017 October 3; revised 2017 October 6; accepted 2017 October 6; published 2017 October 16

The Pierre Auger Observatory carried out a search for ultra-high-energy (UHE) neutrinos above $\sim 10^{17}$ eV using its Surface Detector (Aab et al. 2015a). UHE neutrino-induced extensive air showers produced either by interactions of downward-going neutrinos in the atmosphere or by decays of tau leptons originating from tau neutrino interactions in the Earth's crust can be efficiently identified above the background of the more numerous ultra-high-energy cosmic rays (Aab et al. 2015b). Remarkably, the position of the transient in NGC 4993 was just between $0^{\circ}.3$ and $3^{\circ}.2$ below the horizon during $t_c \pm 500$ s. This region corresponds to the most efficient geometry for Earth-skimming tau neutrino detection at 10^{18} eV energies. No neutrino candidates were found in $t_c \pm 500$ s (Alvarez-Muniz et al. 2017) nor in the 14 day period after it (A. Albert et al. 2017, in preparation).

Pierre Auger can also contribute to
Multi-messenger astronomy

AugerPrime motivation

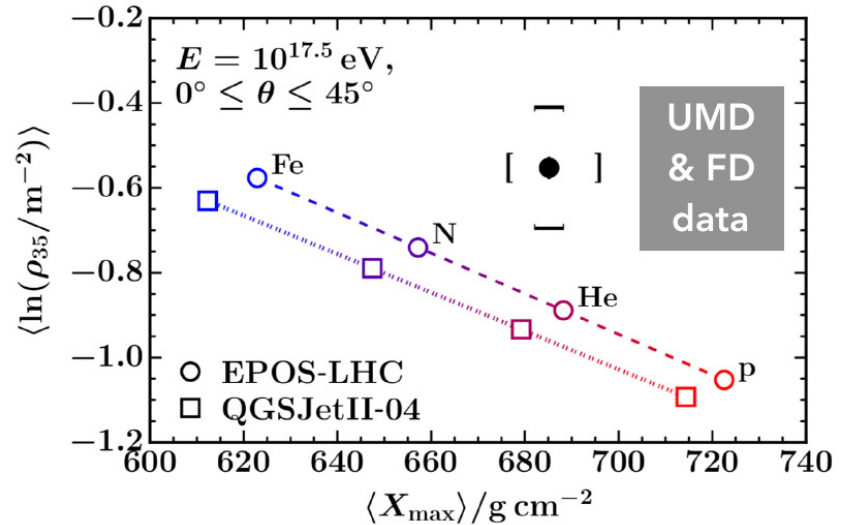
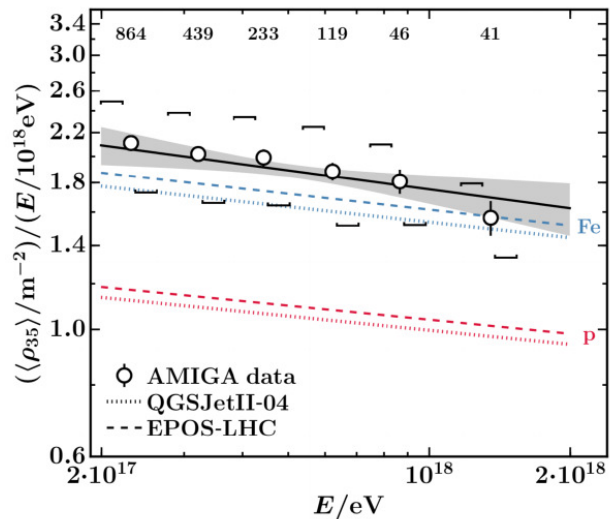
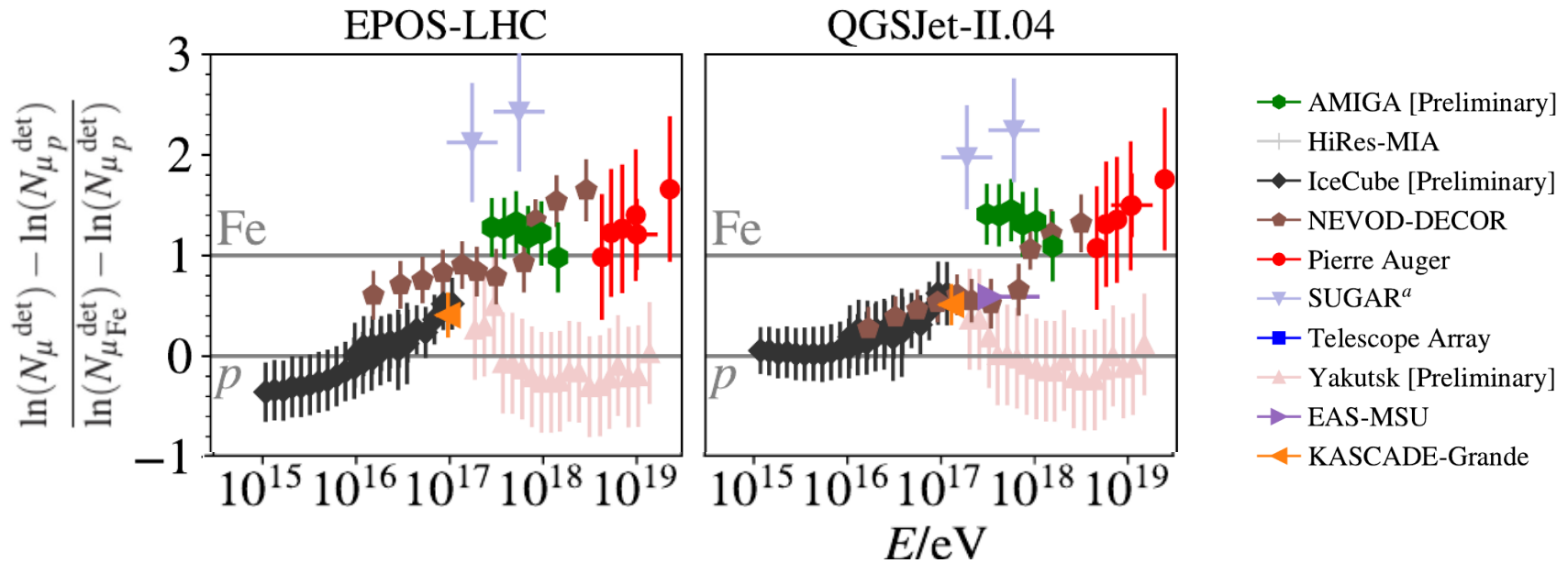
arXiv:1604.03637



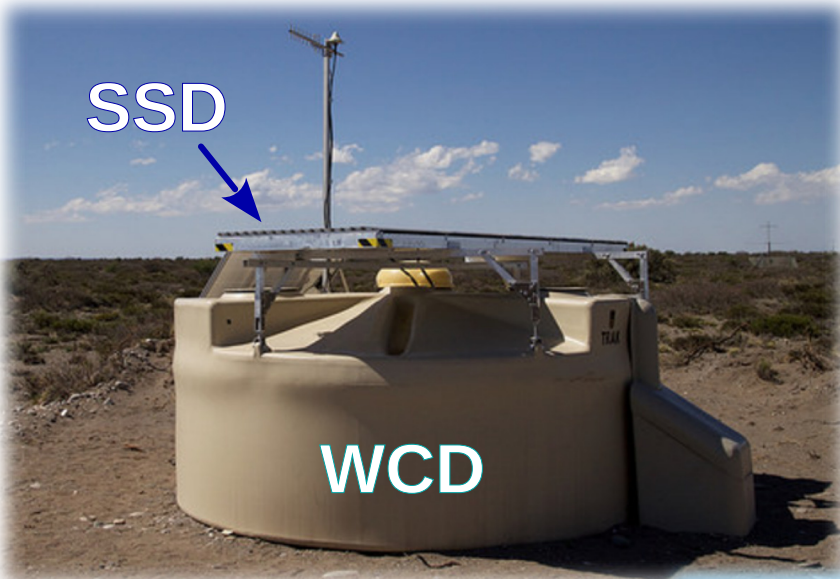
- **Mass composition** cosmic rays with $E > 10^{19}$ eV.
- **Protons** with $E > 10^{19}$ eV.
- **Hadronic models.**

Improve statistics and mass discrimination

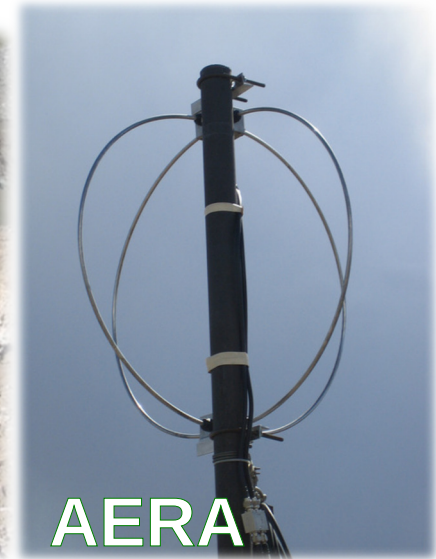
Motivation: muon content in EAS



Upgrade components

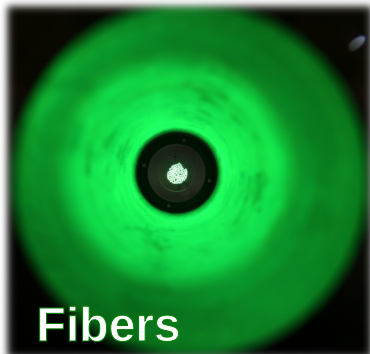
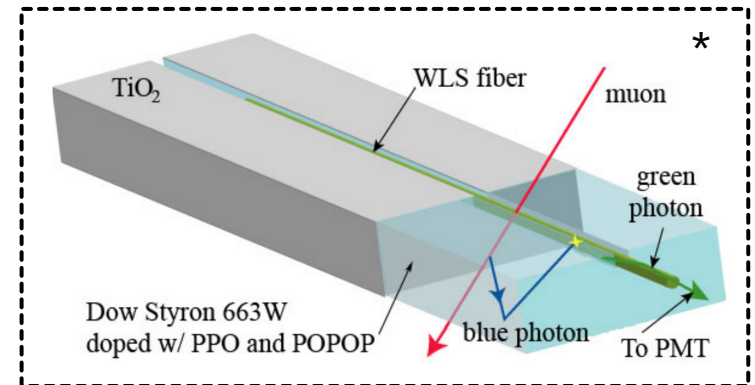


- New electronics for the **WCD**:
 - + resolution, sample time and dynamic range.
- + *duty cycle* del **FD** (de 15 % hasta 30 %).
- Scintillator Surface Detector (**SSD**) over each **WCD** (1500 m).
- Underground Muon Detector (**UMD-AMIGA**) close to each **WCD** (750 and 433 m).
- Auger Engineering Radio Array (**AERA**) over *each* **WCD** (1500 m).



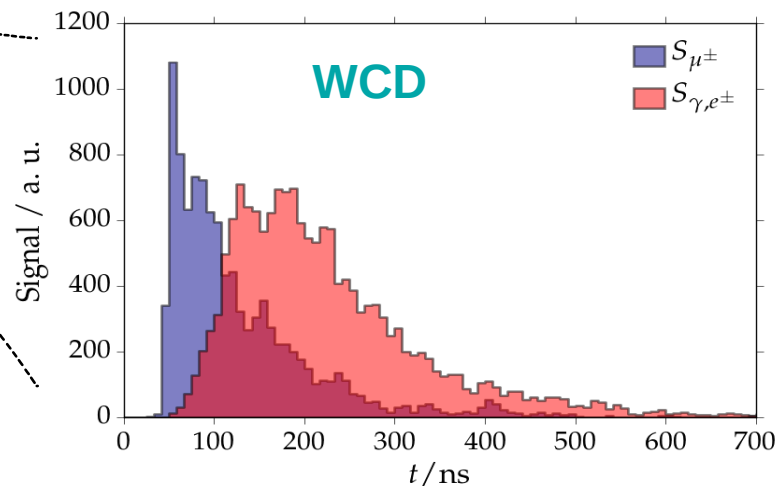
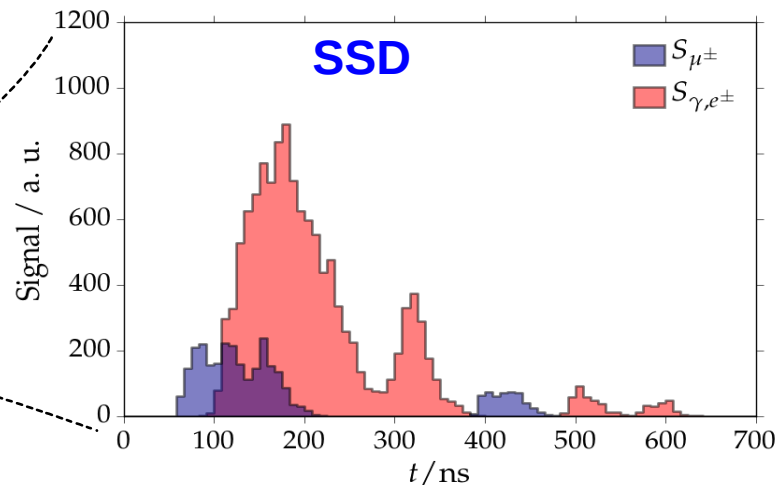
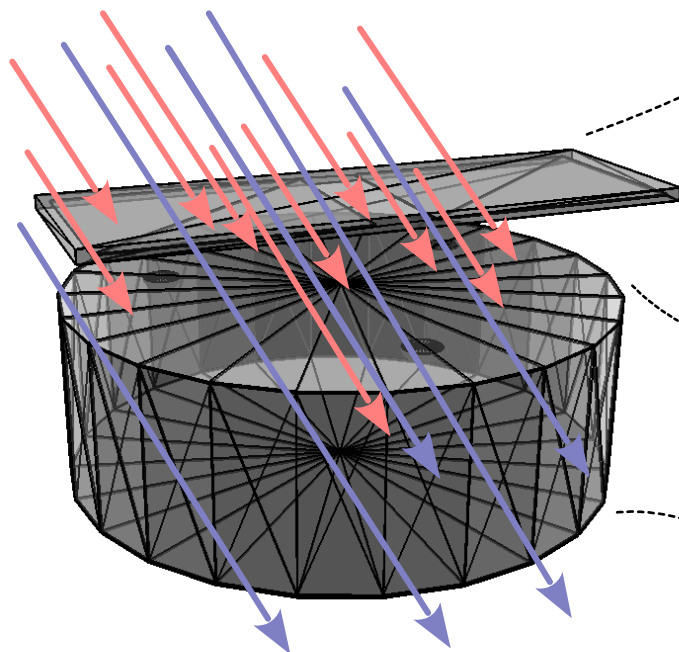
Scintillator Surface Detector (SSD)

- 3.8 m² scintillator
- 48 scintillator strips + WLS optical fiber
- PMT
- Aluminium casing



Scintillator Surface Detector (SSD)

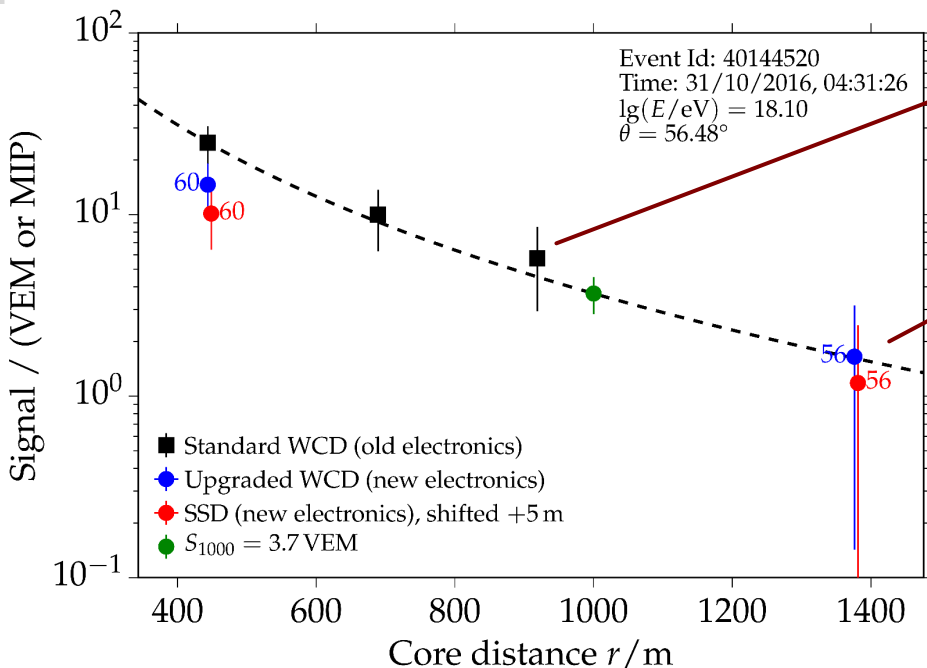
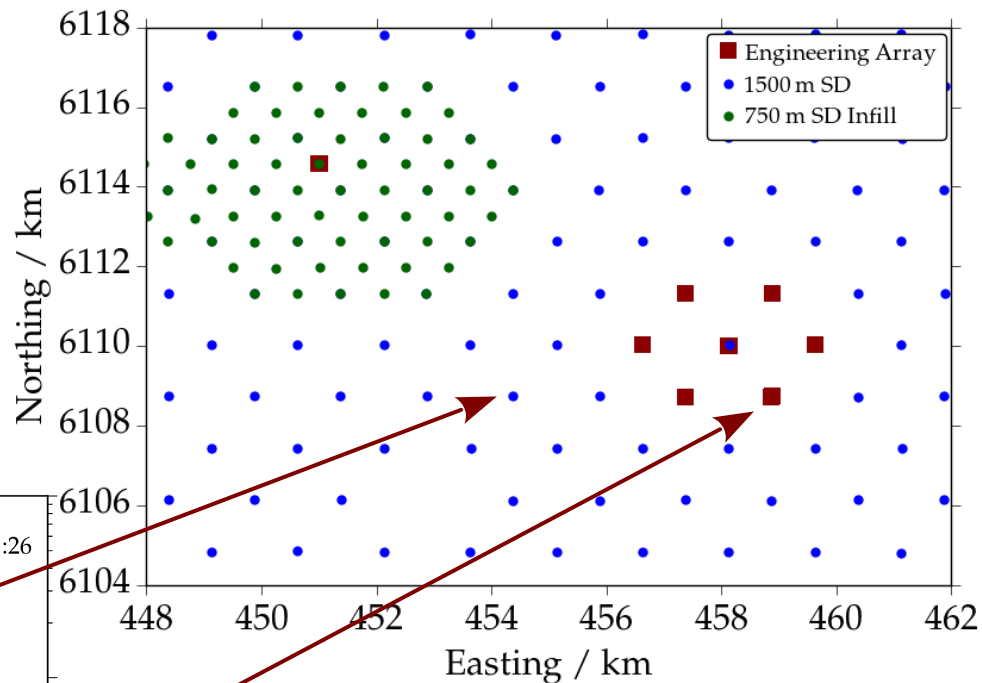
- Complementary response between **SSD** and **WCD**.
- **Electromagnetic** and **muon** separation.



$$S_{\mu, \text{WCD}} = aS_{\text{WCD}} + bS_{\text{SSD}}$$
$$S_{\text{em}, \text{WCD}} = cS_{\text{WCD}} + dS_{\text{SSD}}$$

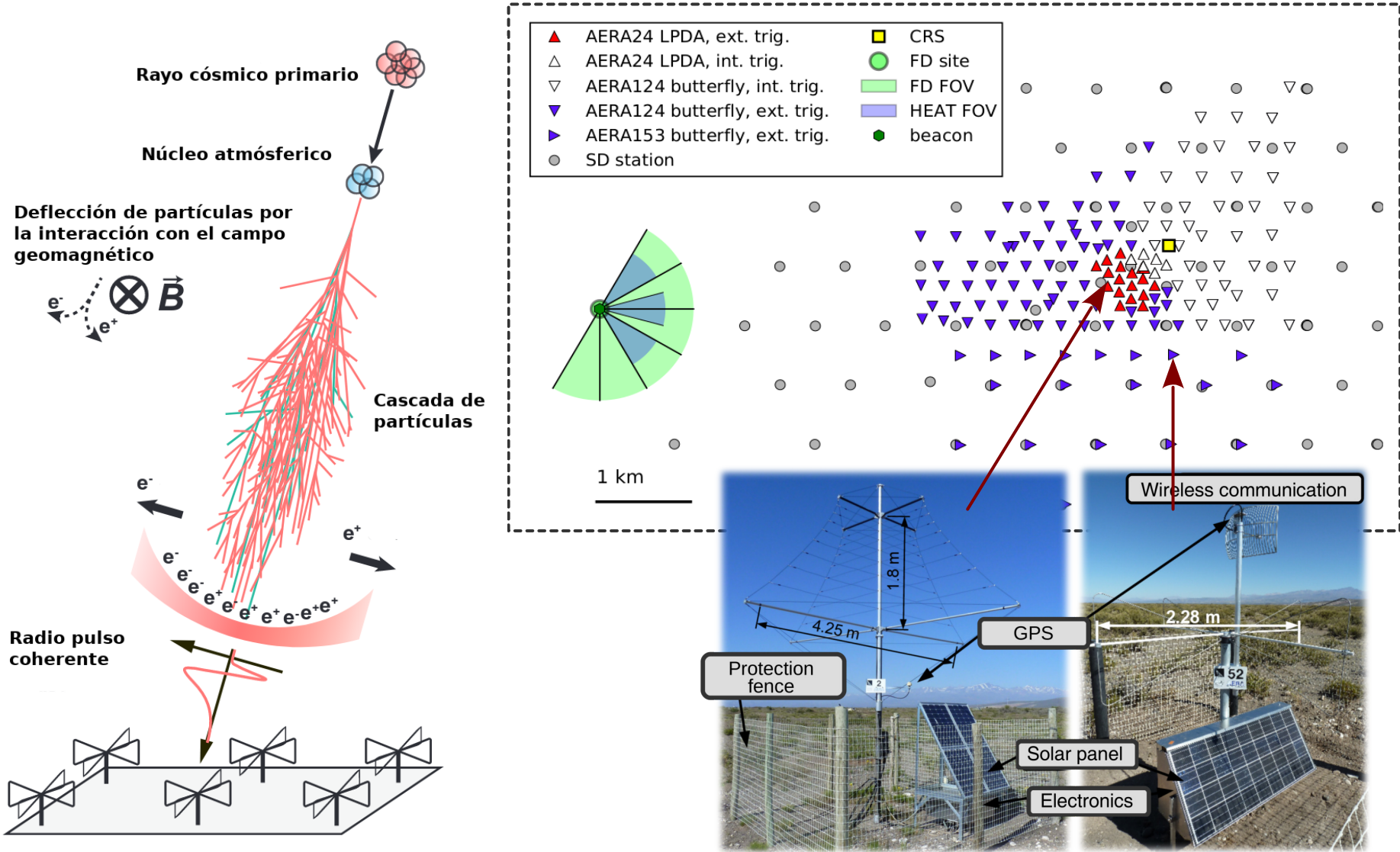
First engineering array data (SSD)

12 SSDs in engineering array.
Acquisition since October 2016.

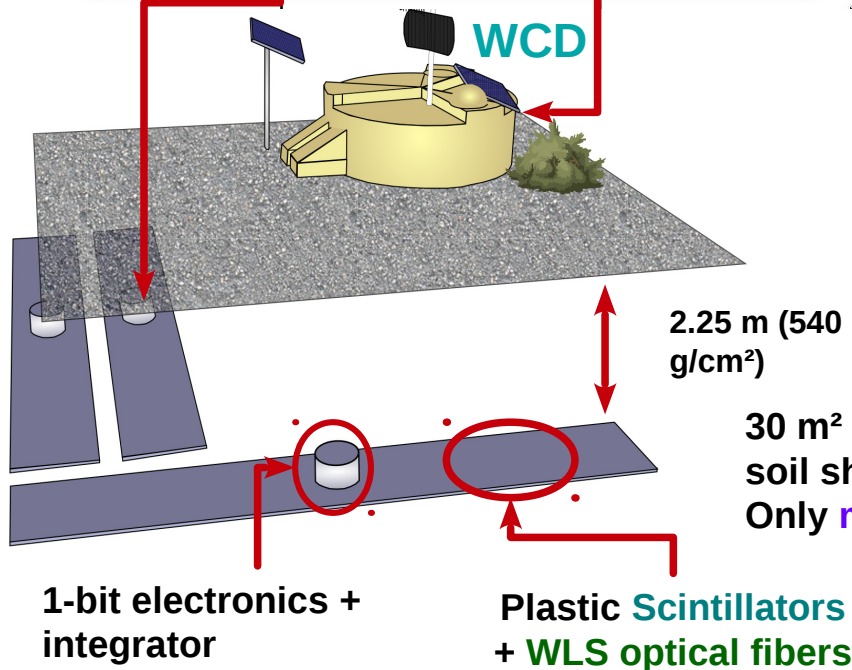
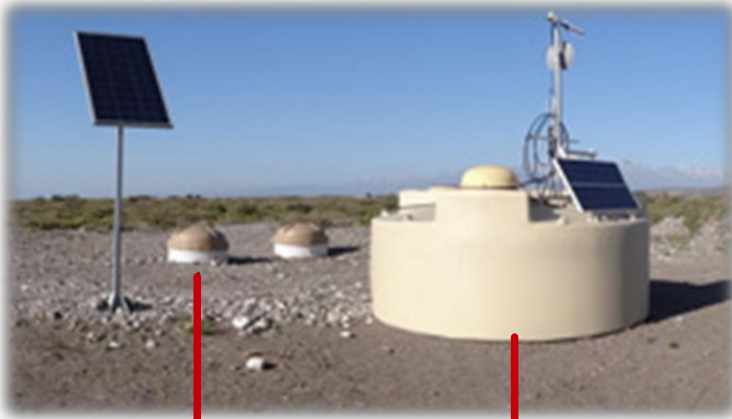


Reconstruction of Lateral Distribution Functions (LDFs) with SSDs and WCDs.

Auger Engineering Radio Array (AERA)



Underground Muon detector (**UMD-AMIGA**)

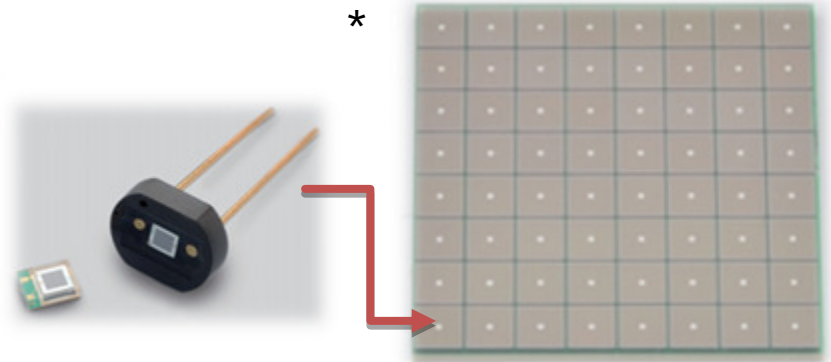


- Infill
- 61 WCD
- SD 750 m
- SD 433 m

Underground Muon Detector (**UMD-AMIGA**)

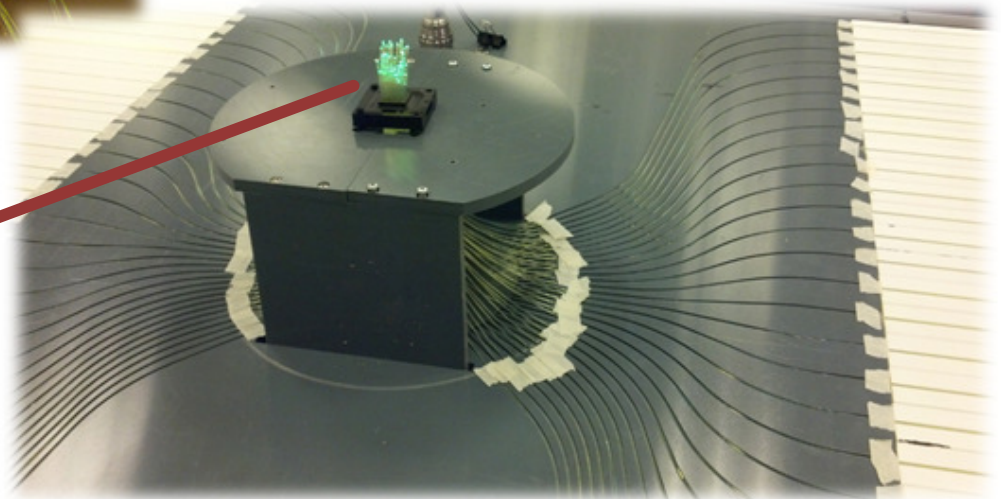


64 **scintillator strips**



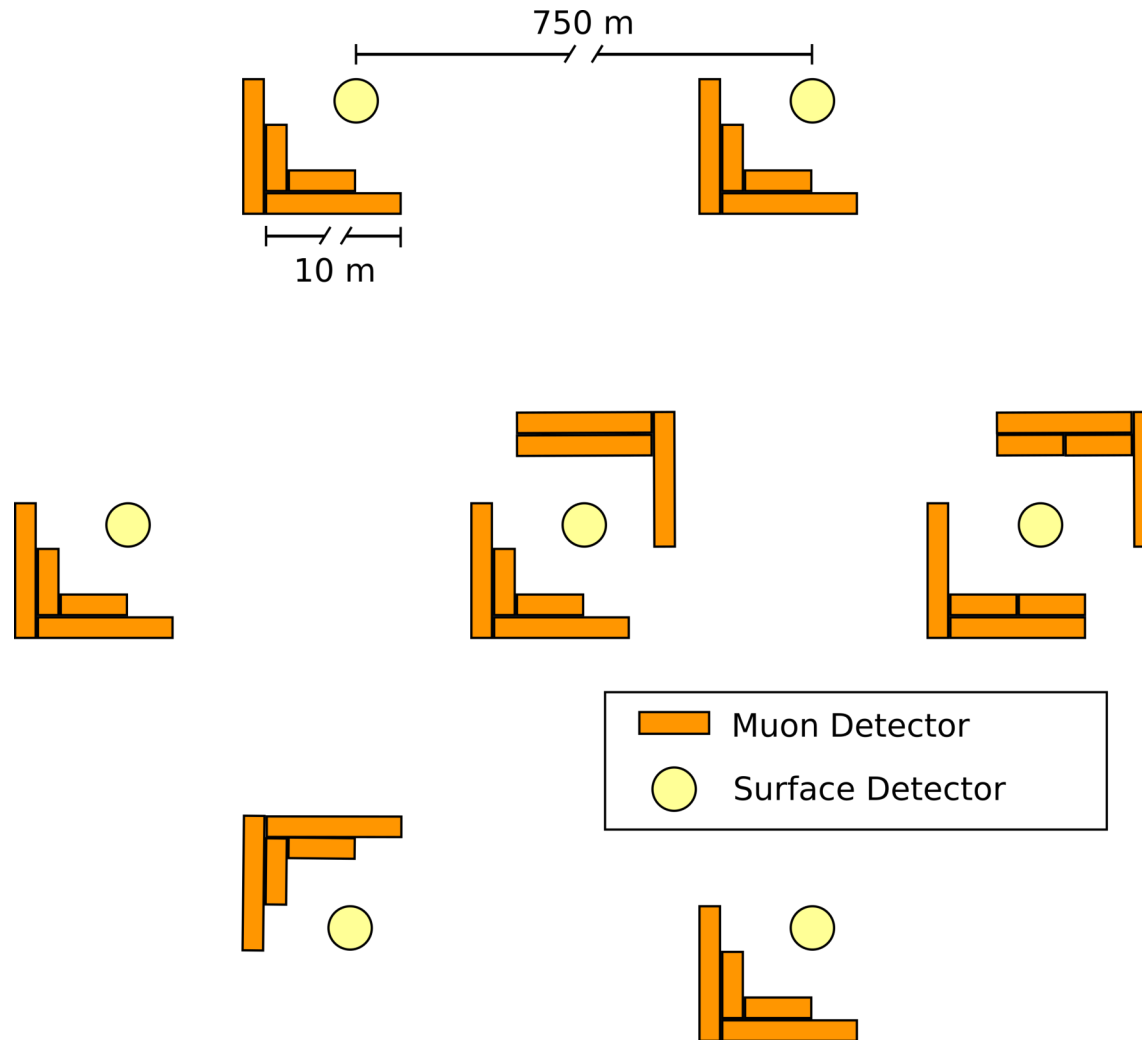
8x8 array of silicon photomultipliers (**SiPM**).

WLS optical fiber

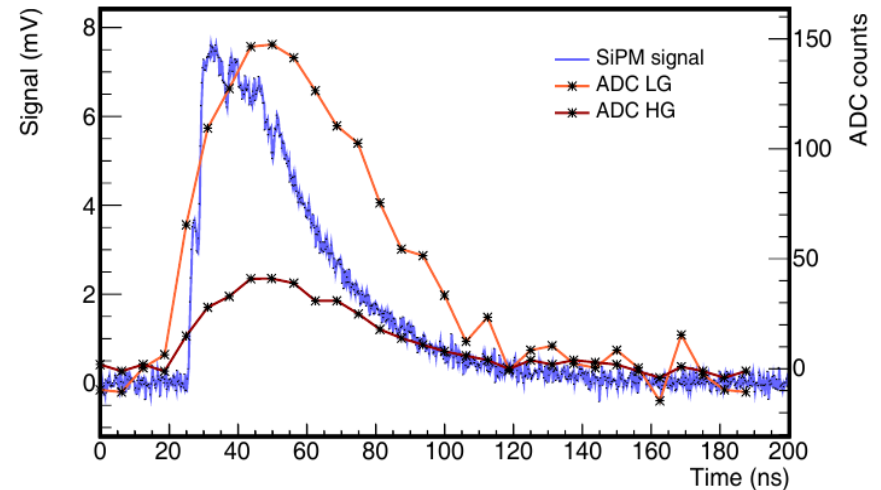
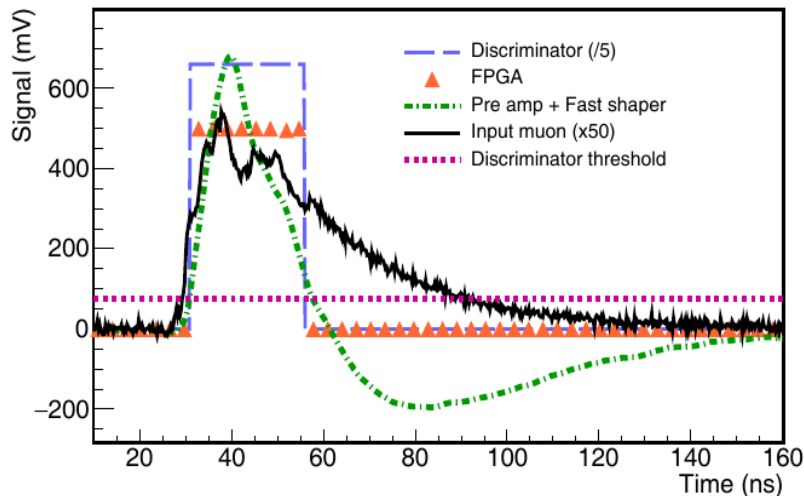
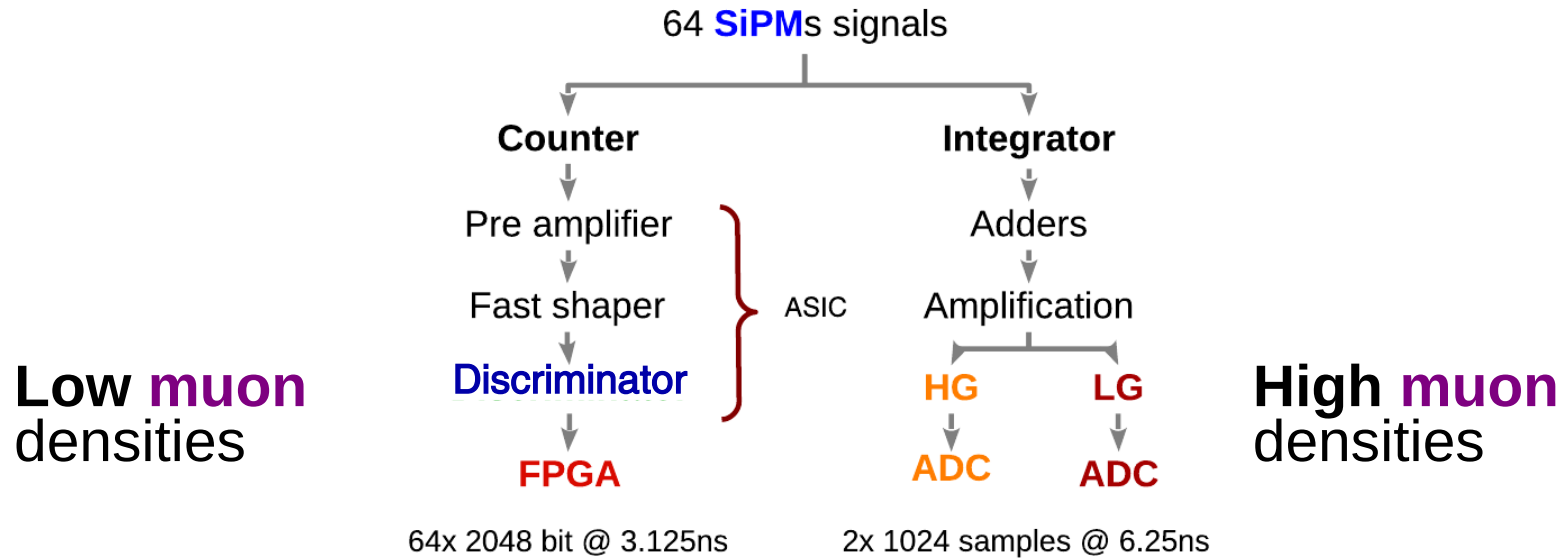


* Picture from Hamamatsu MPPC array S13361-3050NE-08

AMIGA Engineering array



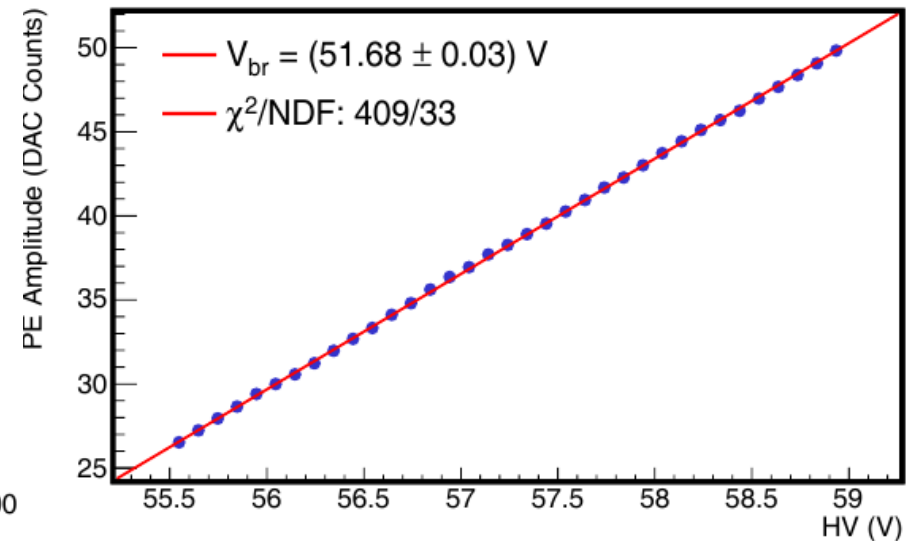
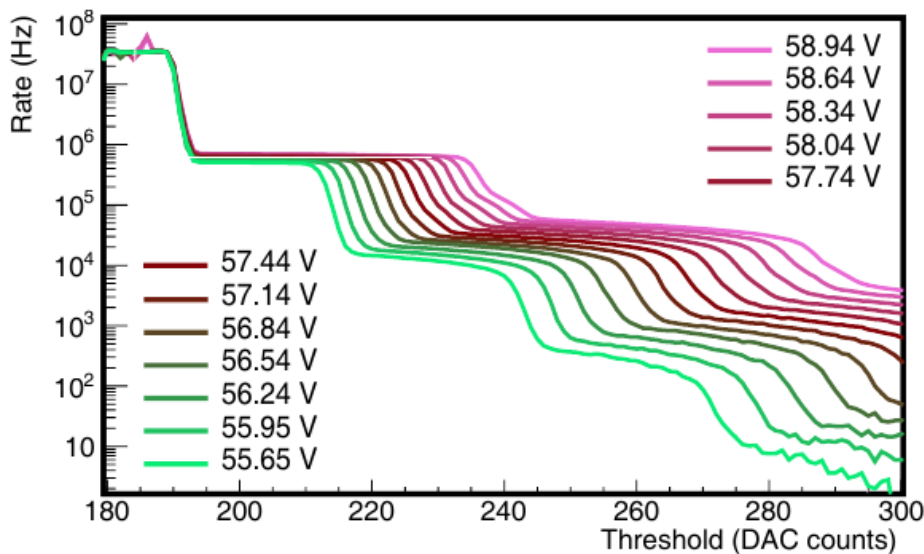
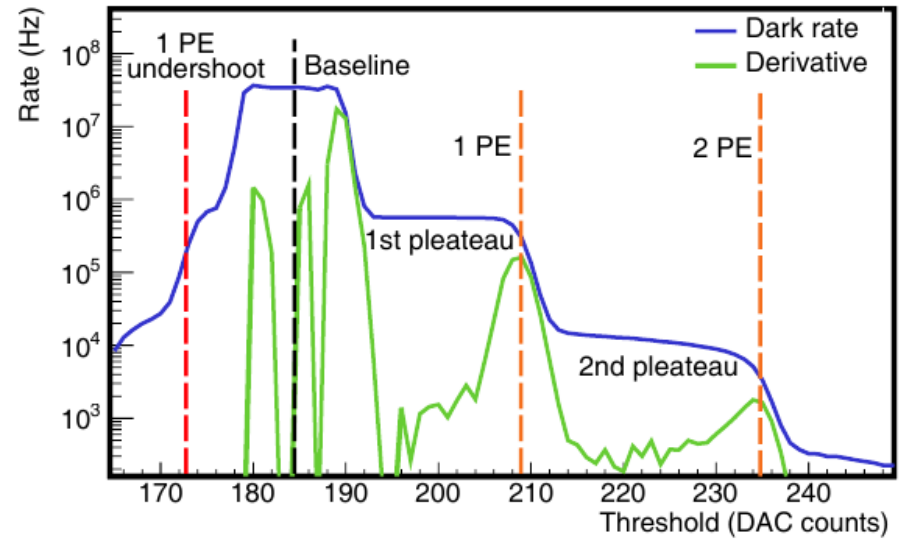
UMD-AMIGA Electronics



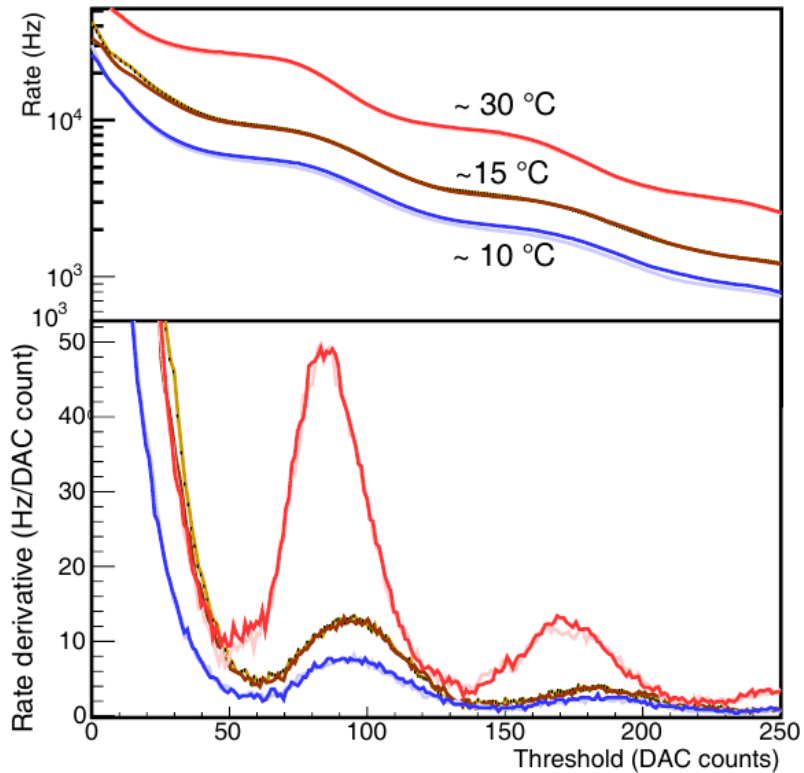
SiPM Calibration

Goal: obtain **breakdown voltage, V_{br}** , (minimum voltage to operate in Geiger mode).

SiPM gain $\sim HV - V_{br}$

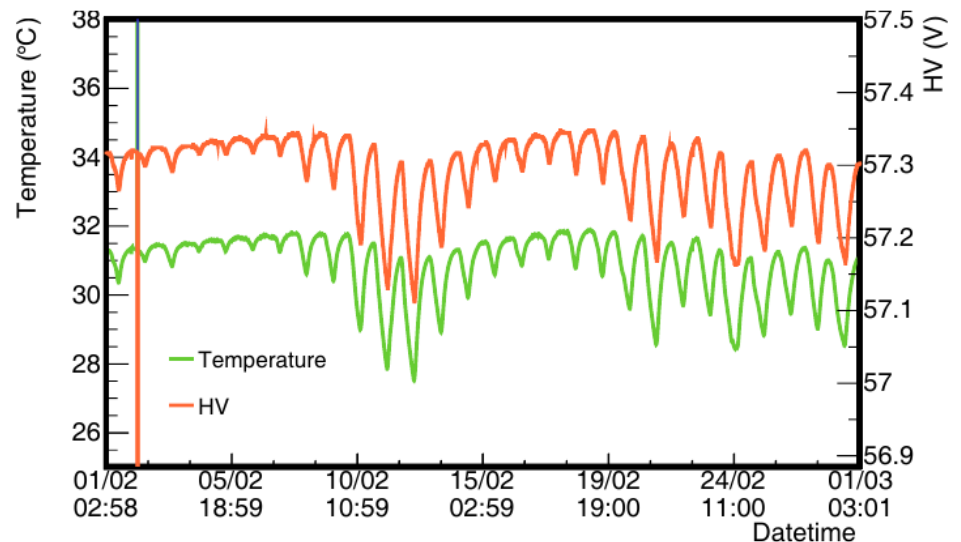
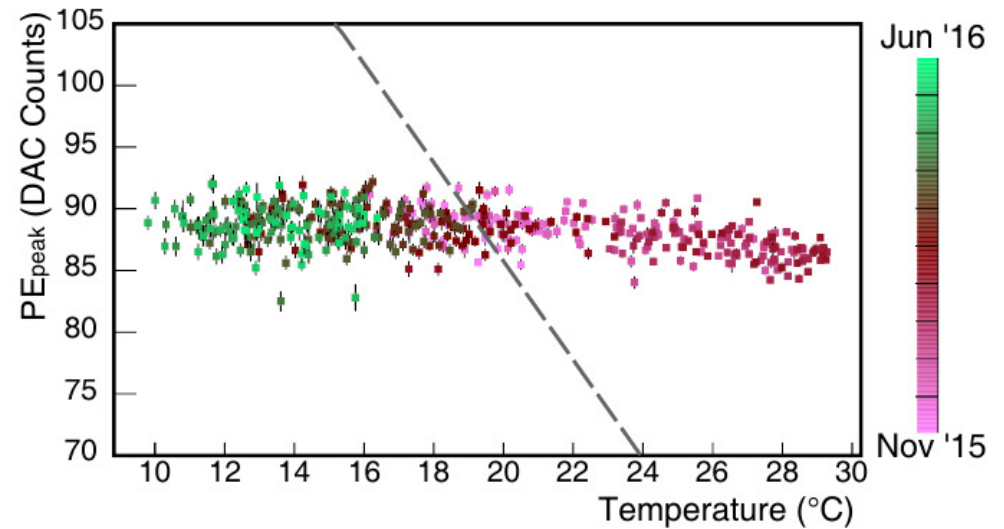


SiPM Temperature dependance

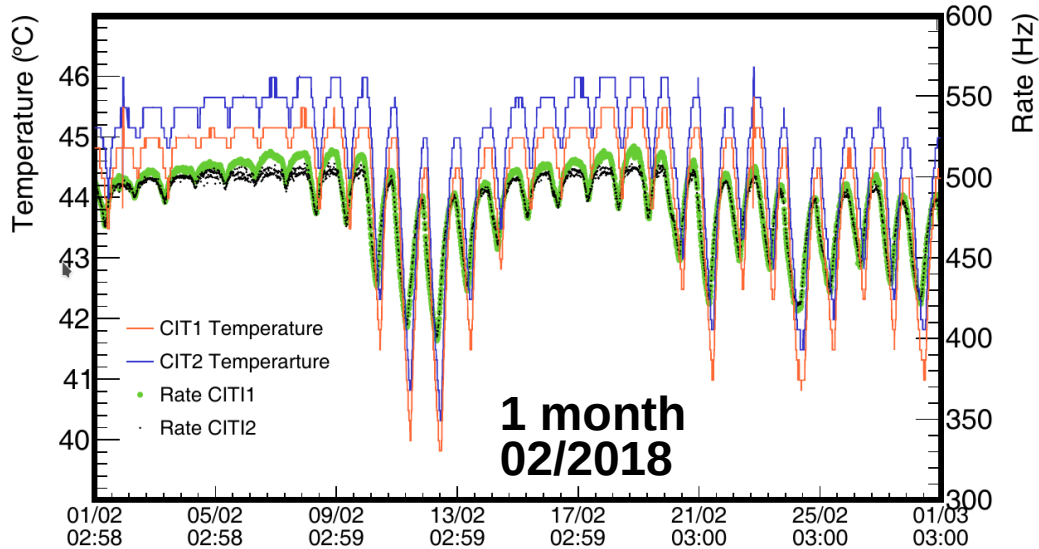


Breakdown voltage depends on Temperature.

HV compensation.

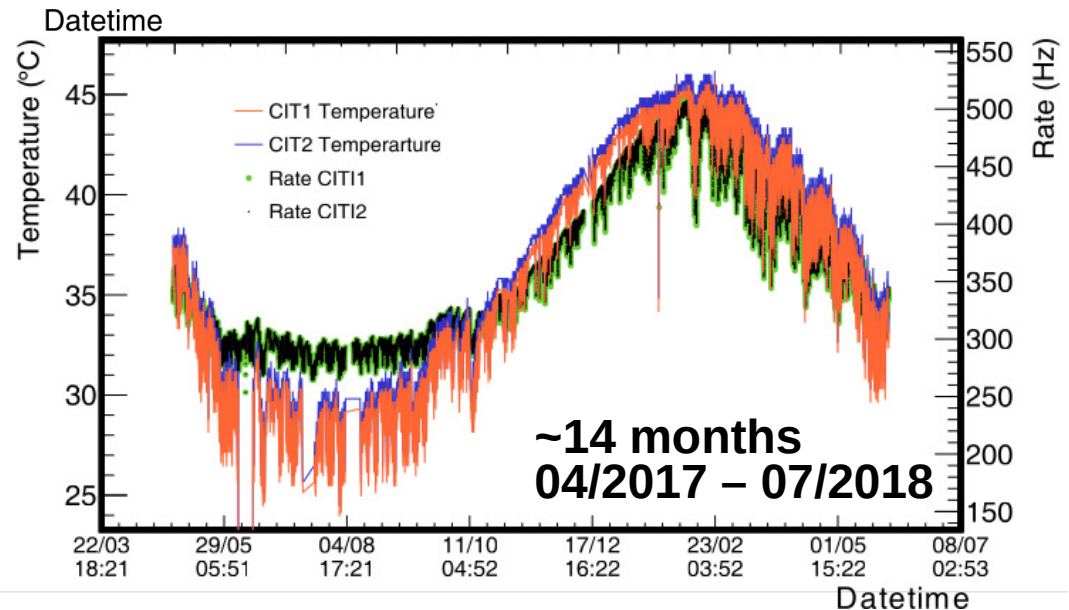


Noise in the field

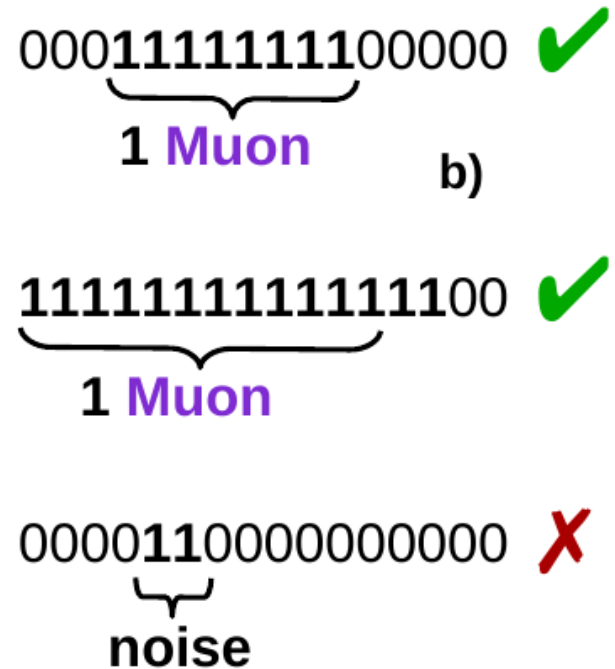
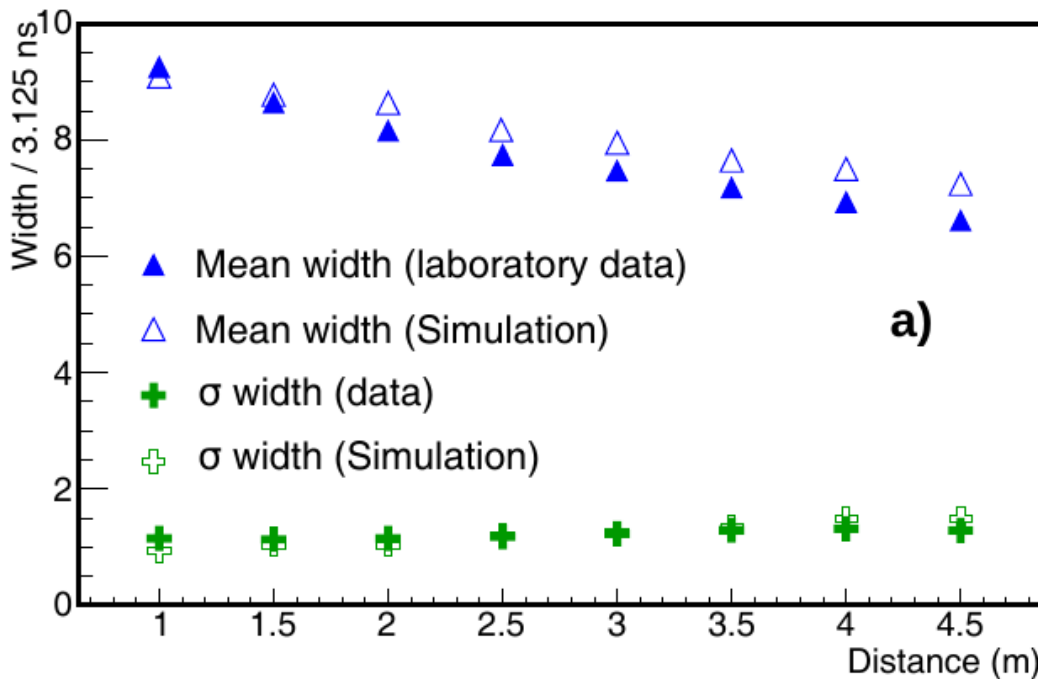


- Monitoring data:
- Threshold @ **2.5 PE**
 - Pattern **1x**
 - **6.4 μ s** trace

(10-20) % probability of over-counting 1 muon in 1 event per module (In the lab: **14.6%**). It can be reduced to **5.5 %** with **1111x** pattern.



Muon counting and noise rejection



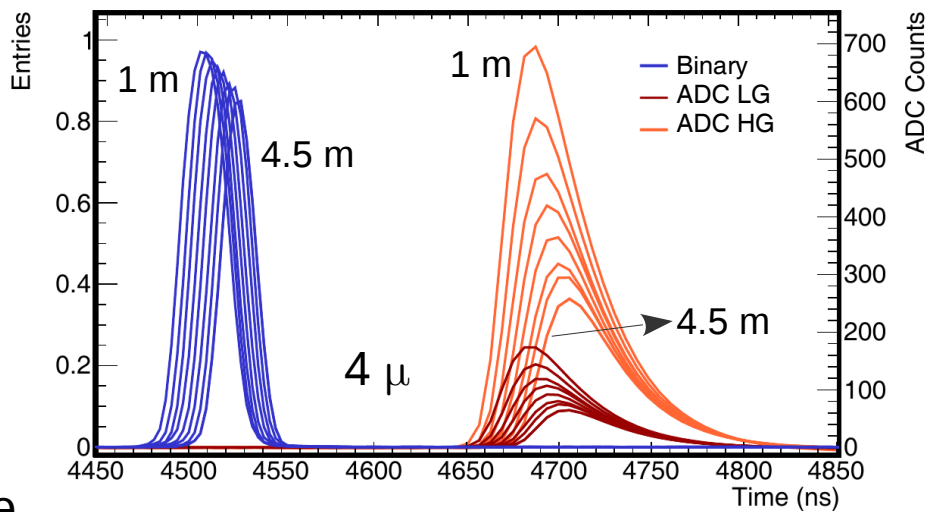
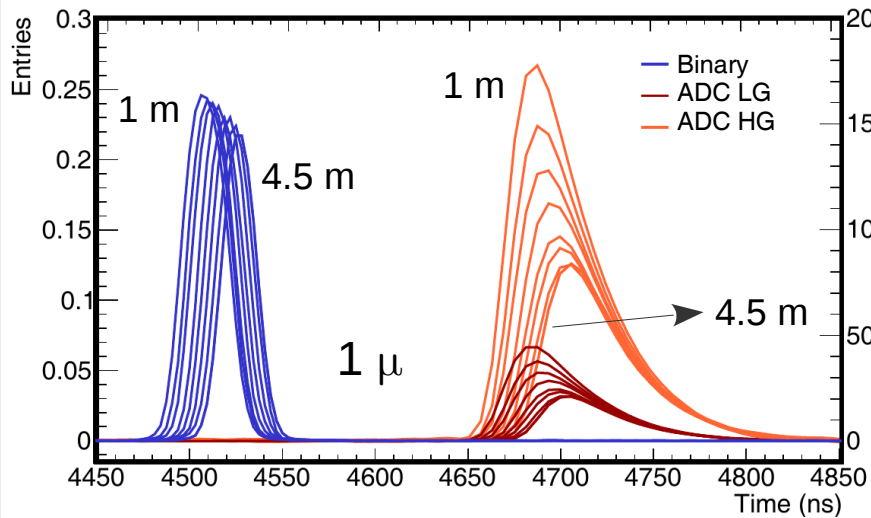
Muon signal width: $\mu = 24.4$ ns and $\sigma = 4.3$ ns.

3 photon-equivalent (PE) dark rate: < 12.5 ns.

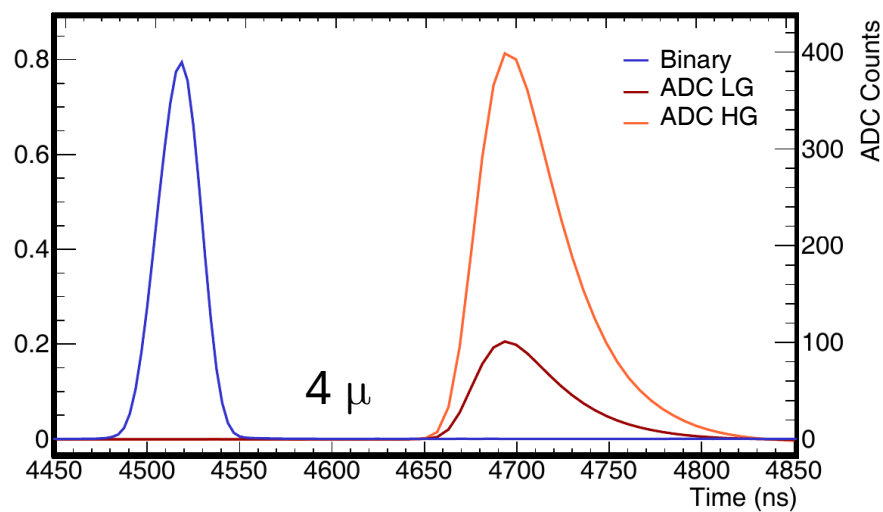
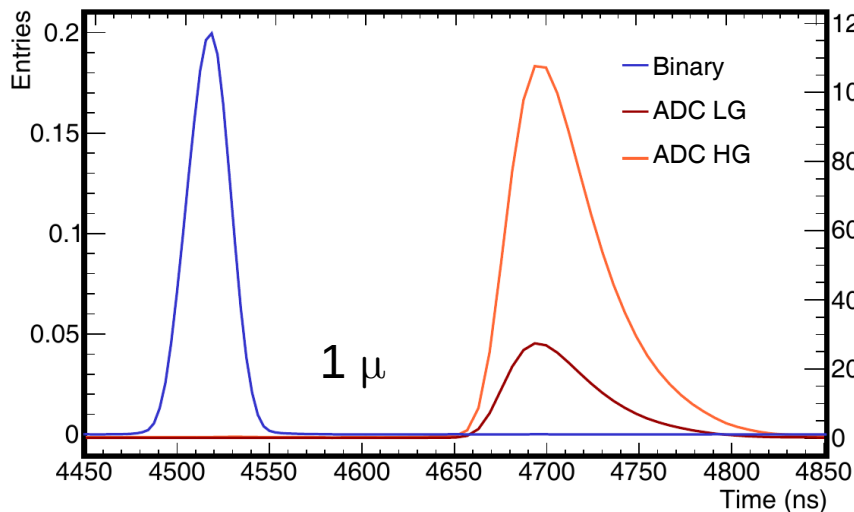
Strategy: a **muon** has between **4** and **12** positive samples.

Counting strategy \rightarrow reduces background by a factor of ~ 2.7 .

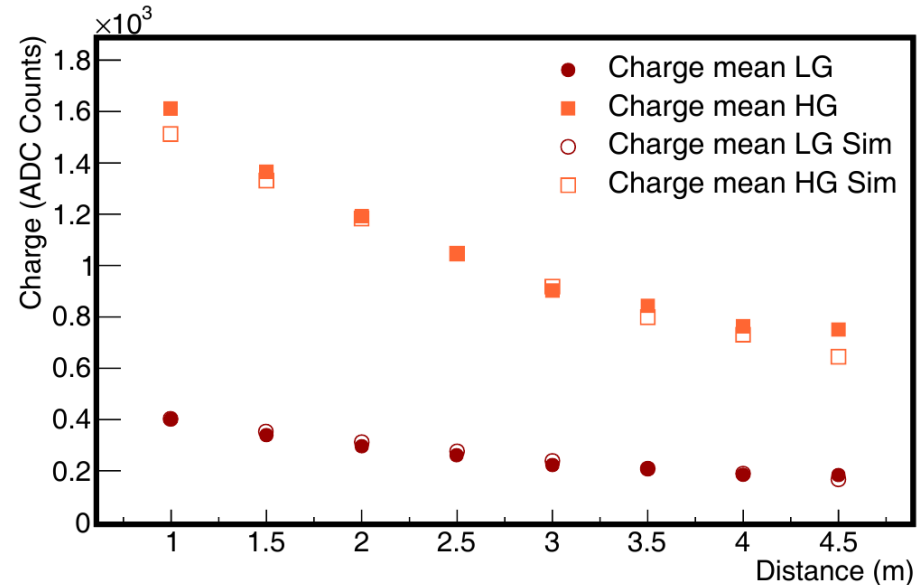
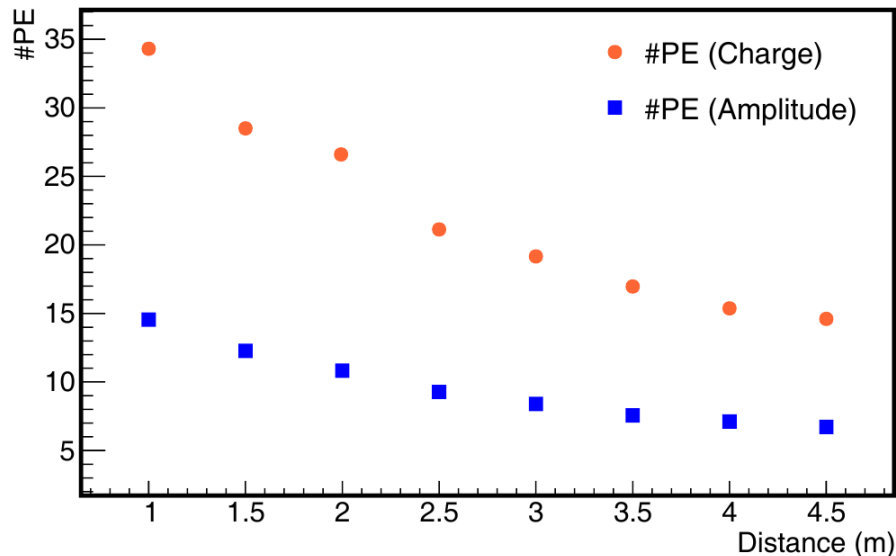
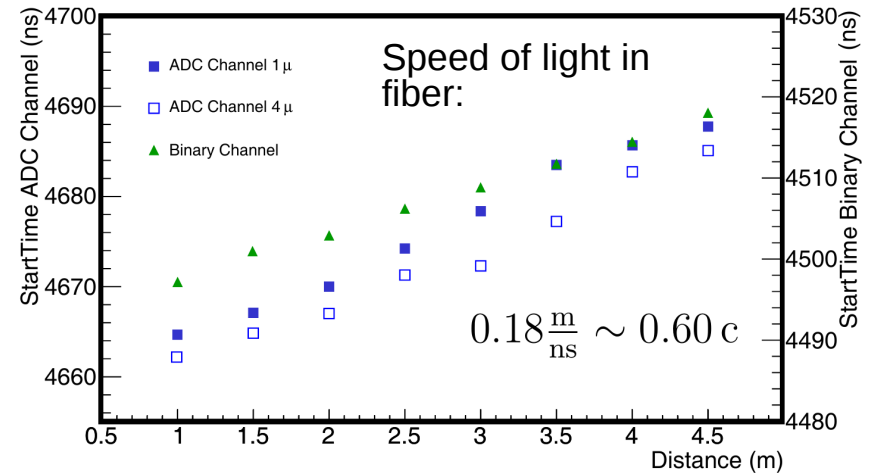
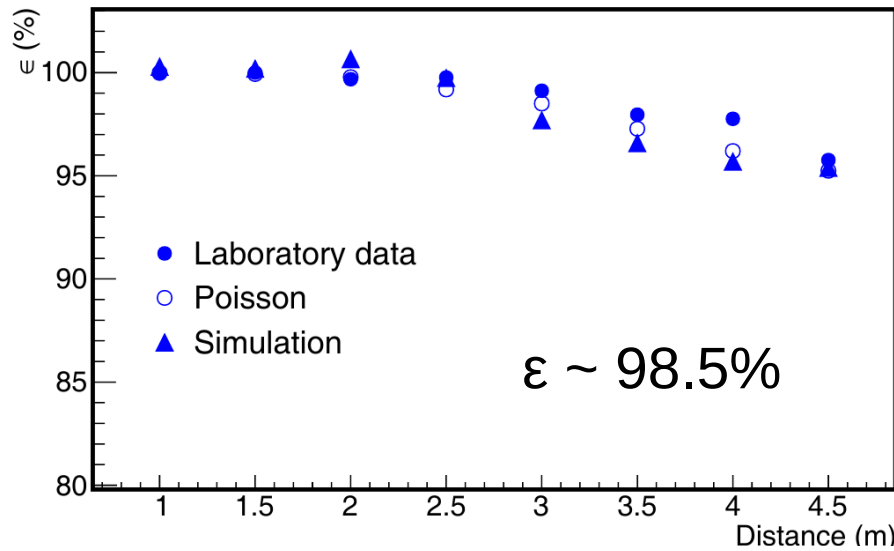
Binary/ADC traces



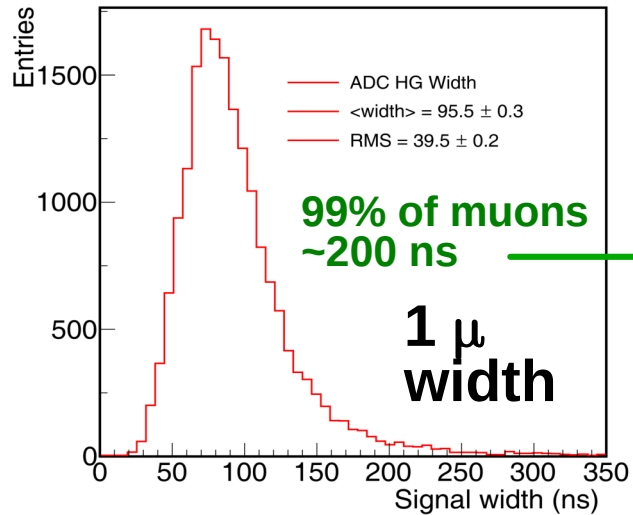
ete



Efficiency and attenuation

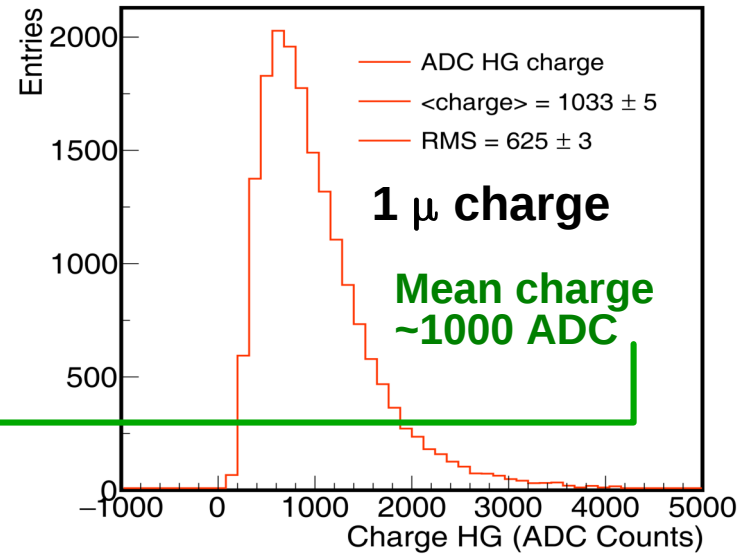
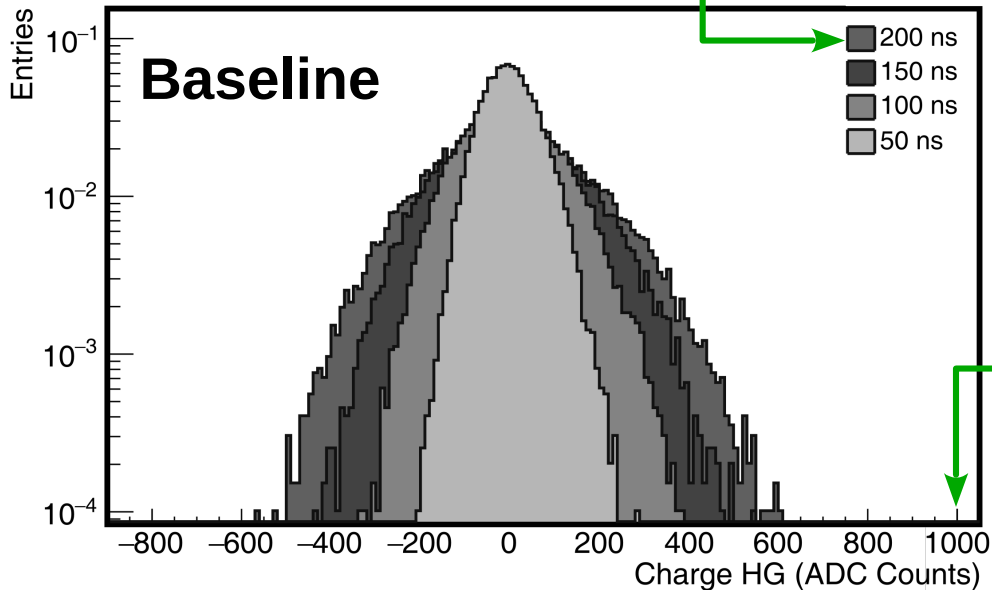


Muon **ADC** signal in LAB*



MIP separated from baseline.

In **LAB**, events triggered with background muons.

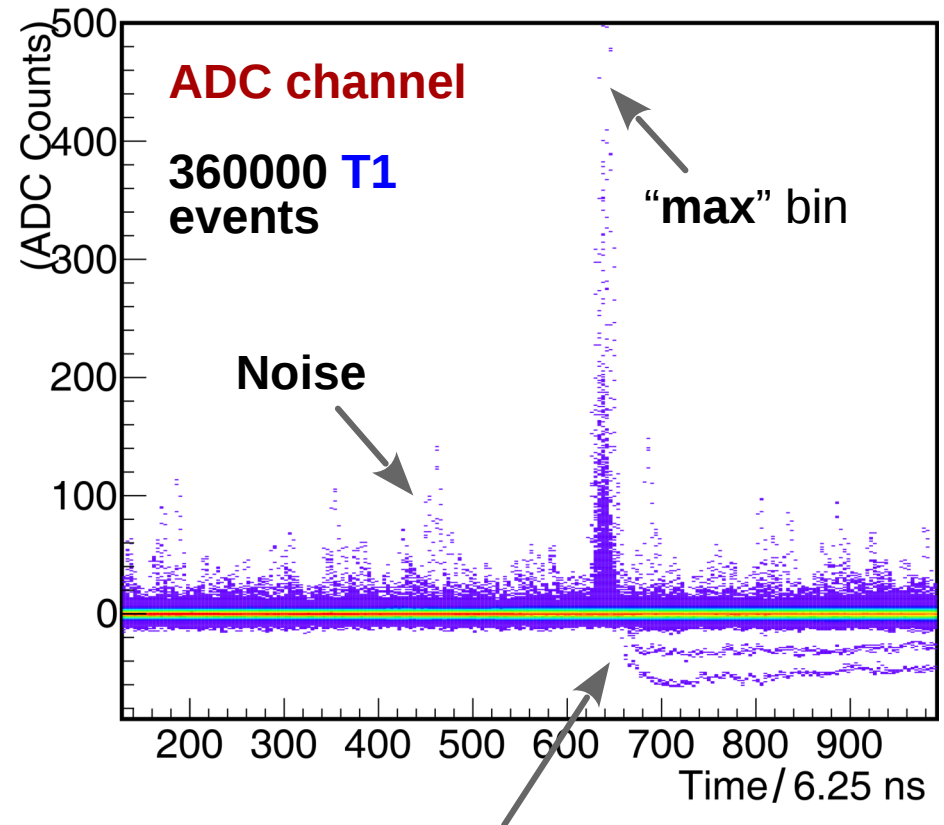
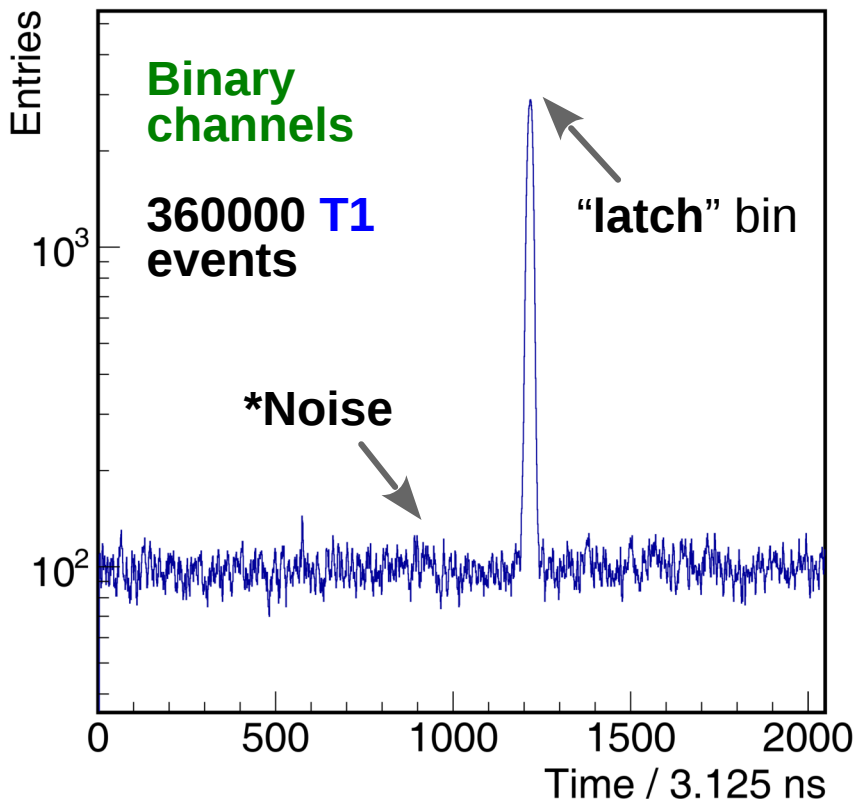


ADC calibration in the field

Online calibration using background data?

- Muon detector triggered with **WCD T1** (mostly background muons).
 - **T1** events in muon detector **mostly** baseline.
 - **T1s** are not stored (data sent on **T3** request).
-
- Station **93** (Corrientes), module **101**. Out of acquisition since **24-08-2018**.
 - Stores one **T1** event per second (**1 Hz**).
 - Data set: **360000** events \equiv 1 hour of all **T1s** (**100 Hz**).
 - Use **binary channel** to separate signal from noise in **ADC**.

T1 Binary/ADC traces

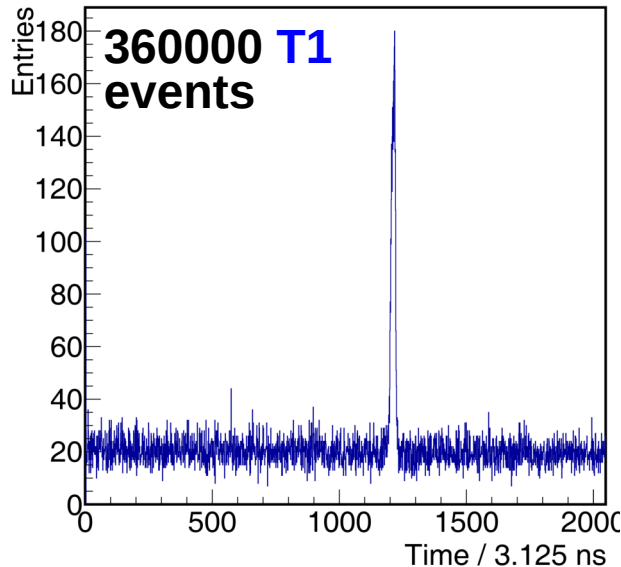


Undershoot (more than one muon)

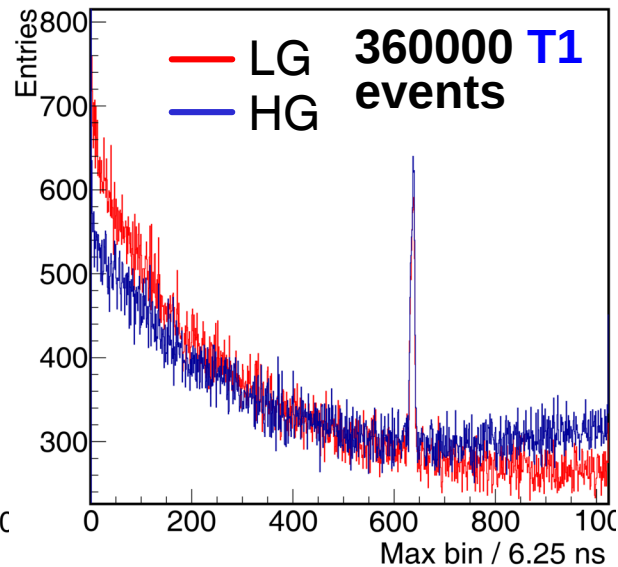
Note time shift between **binary** and **ADC** signal.

T1 Binary/ADC time shift

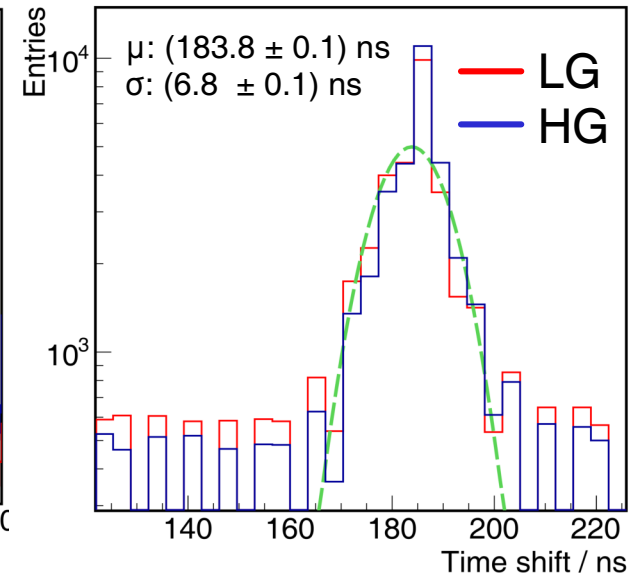
Binary channels
star time (1st one
in trace):



ADC channel
maximum signal bin:



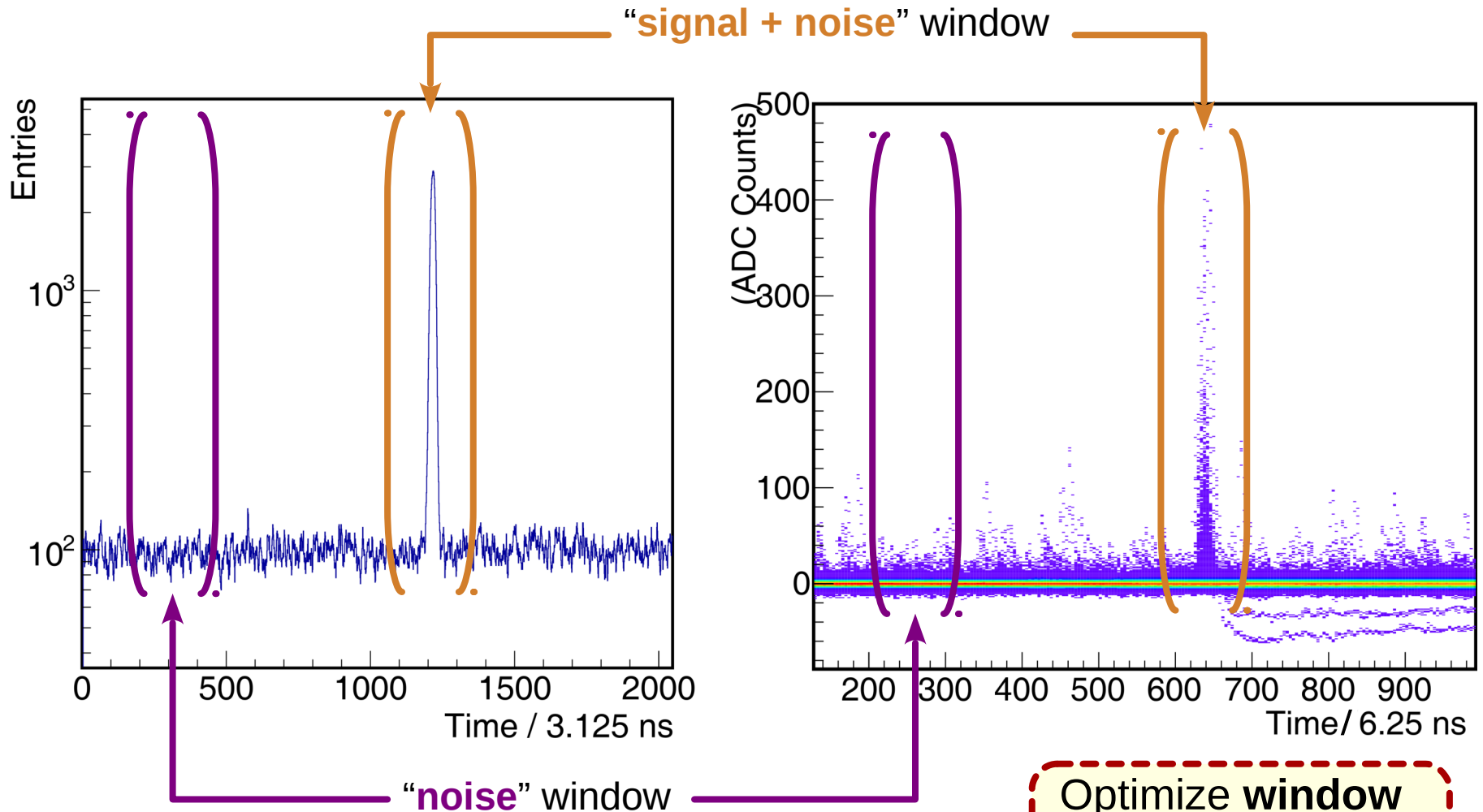
Time shift:



Signal **cuts** (1 muon \rightarrow lab data) :

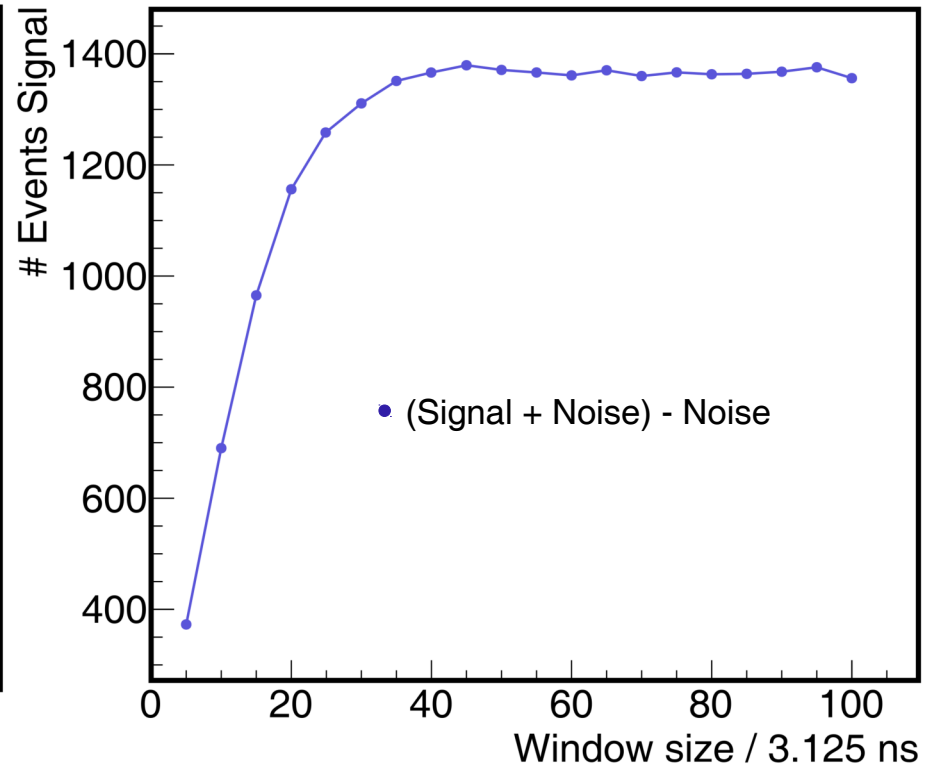
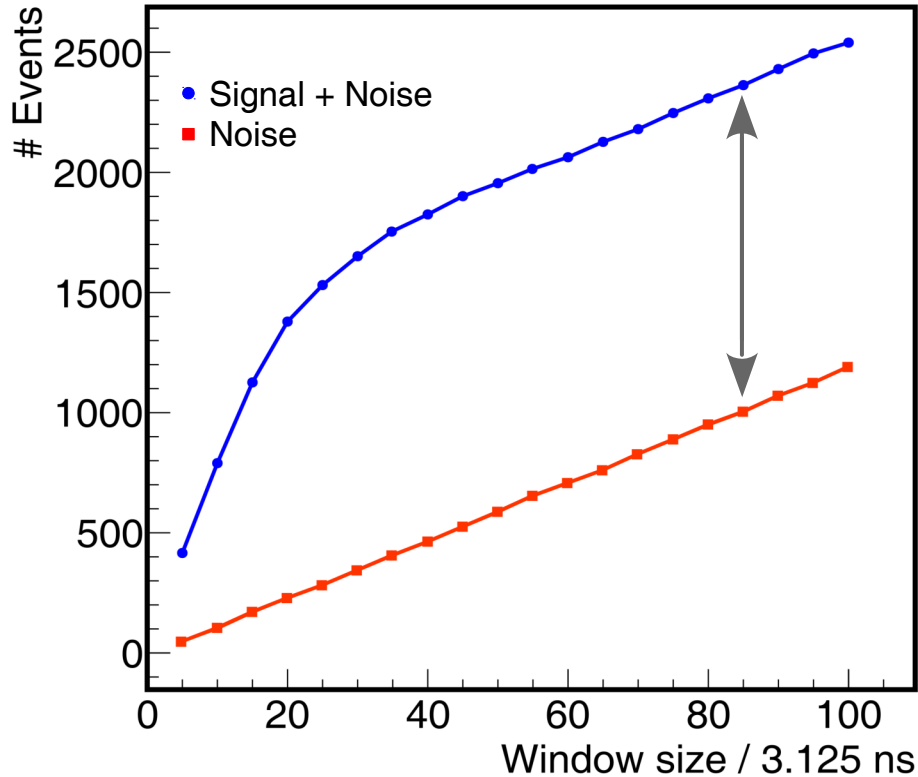
- \rightarrow **1111x** pattern.
- \rightarrow **< 12** positive samples.
- \rightarrow **1 channel on.**

T1 Binary/ADC traces



Optimize **window** size around **binary** latch.

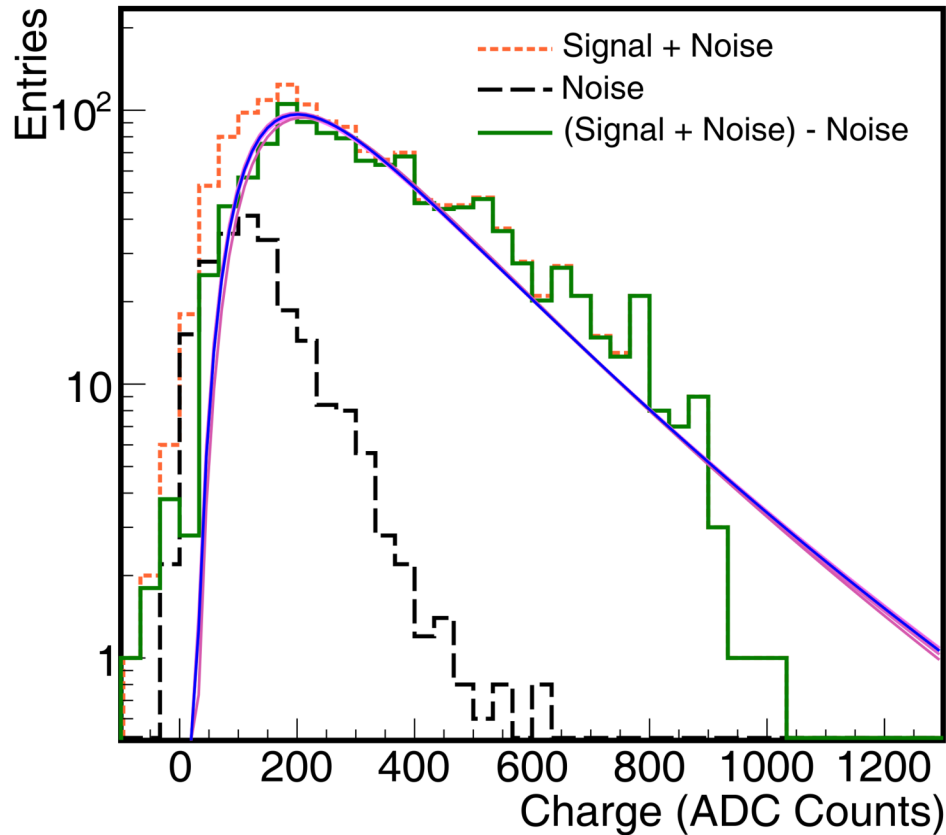
T1 number of events



~40 bin window
contains all signal
events

T1 calibration histograms

20-bin window



Calibration histogram **built** from **T1** data.

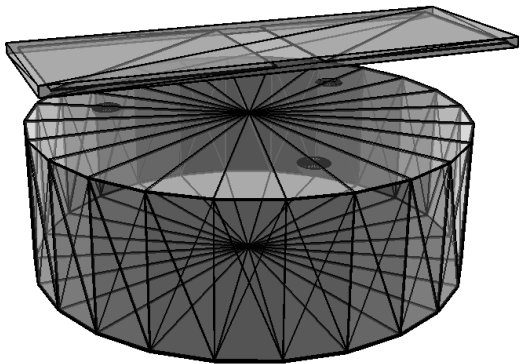
Lognormal fit.

Mean: (358 ± 7) ADC Counts

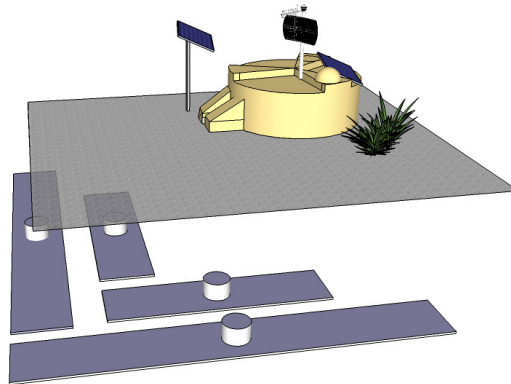
Conclusion

New detectors \longrightarrow improve mass discrimination

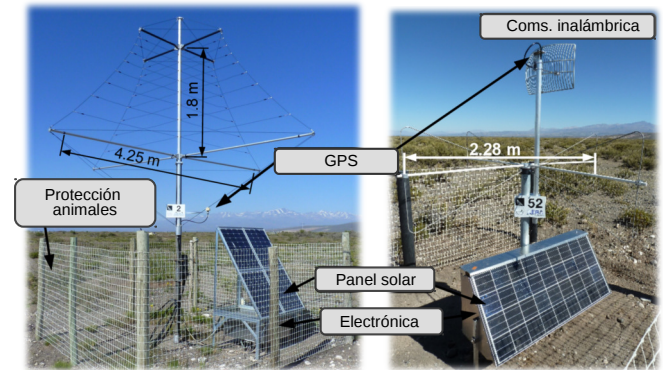
SSD (μ , em)



UMD-AMIGA (μ)



AERA (em)



Increase **FD** duty cycle

\longrightarrow + X_{\max} statistics

New **electronics WCD**

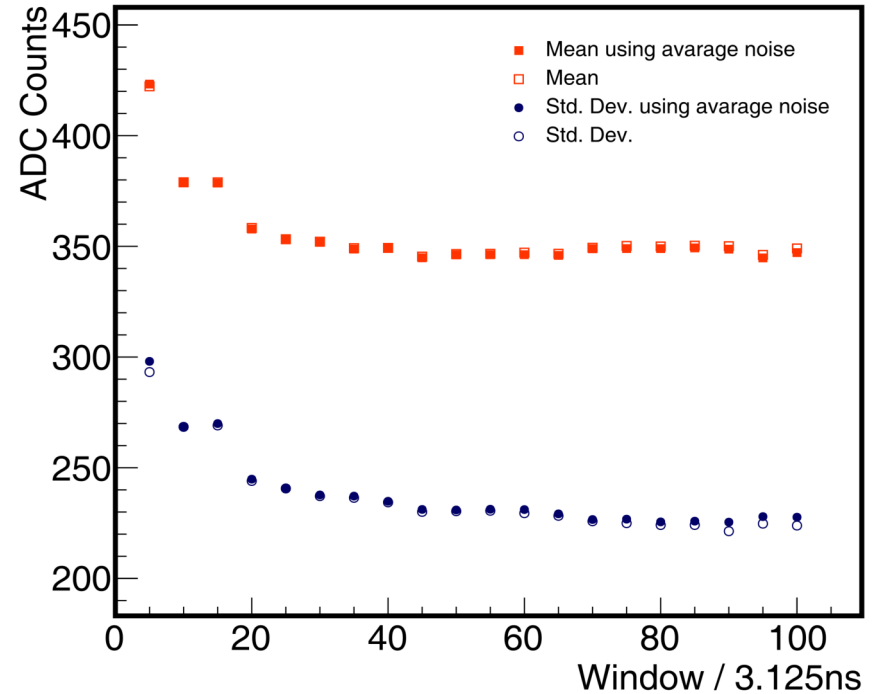
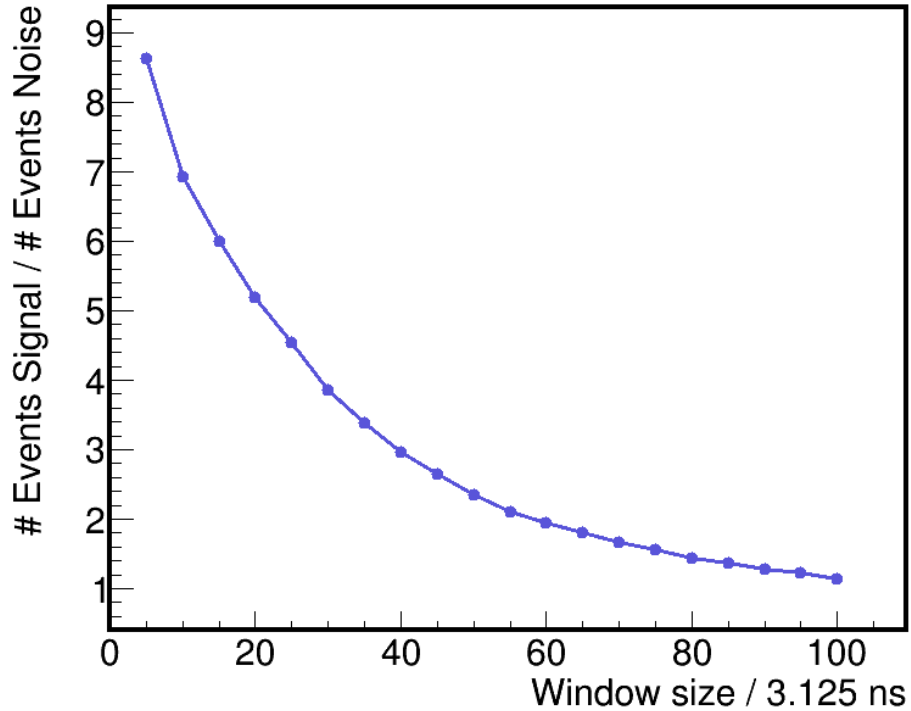
\longrightarrow + sampling speed, resolution and dynamic range.

Conclusions

- Fully characterized **binary** and **ADC** traces.
- **SiPM** calibration achieved.
- Temperature compensation working.
- Muon counting strategy to reduce background.
- **ADC** calibration with **T1** possible (already implemented in electronics!).
- **Online** calibration every **hour** could be achieved.
- Compatible with **offline** calibration with **T3**.
- **Consistent** for different matching **patterns**.
- **Stable** in current range (**24-08-2018** to **02-03-2019**).

BKP

T1 Signal / Noise

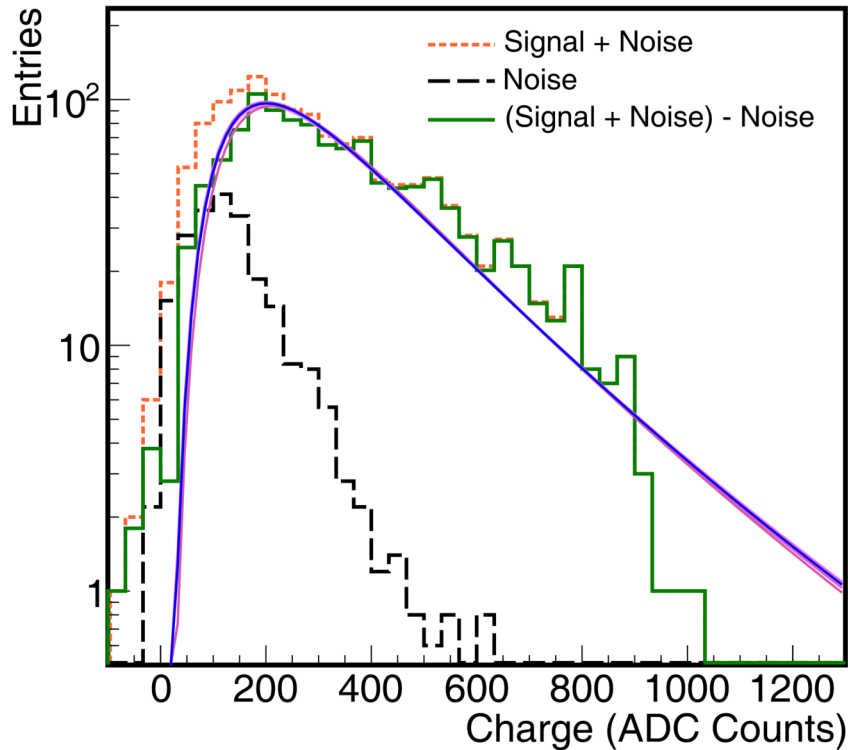


Mean stable @
~ 20 bins

T1 vs T3 calibration

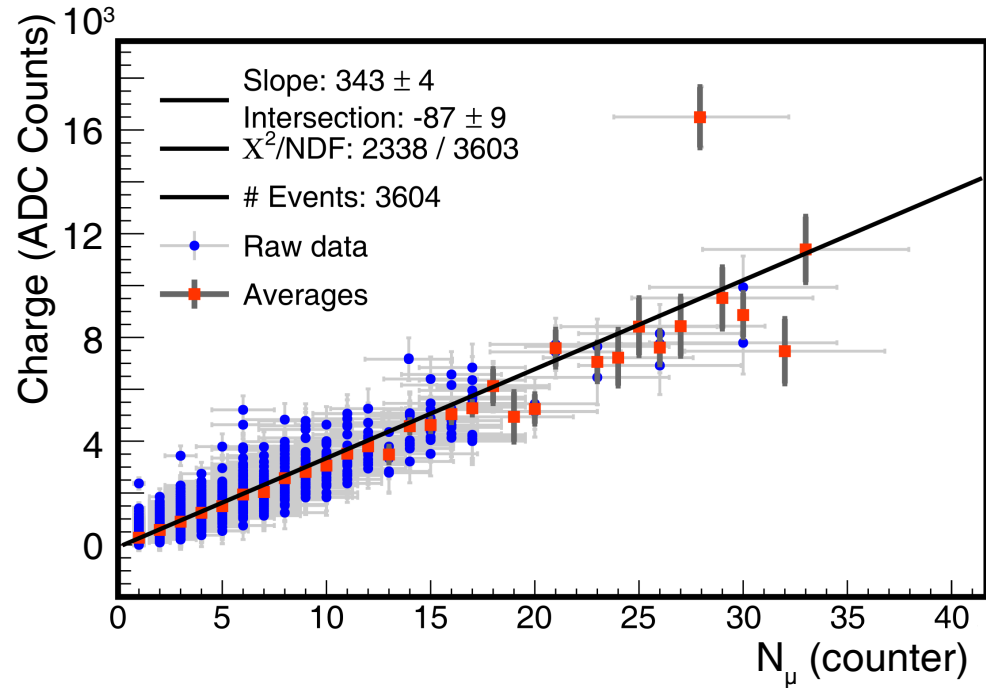
T1/T3
calibrations
consistent

20-bin window



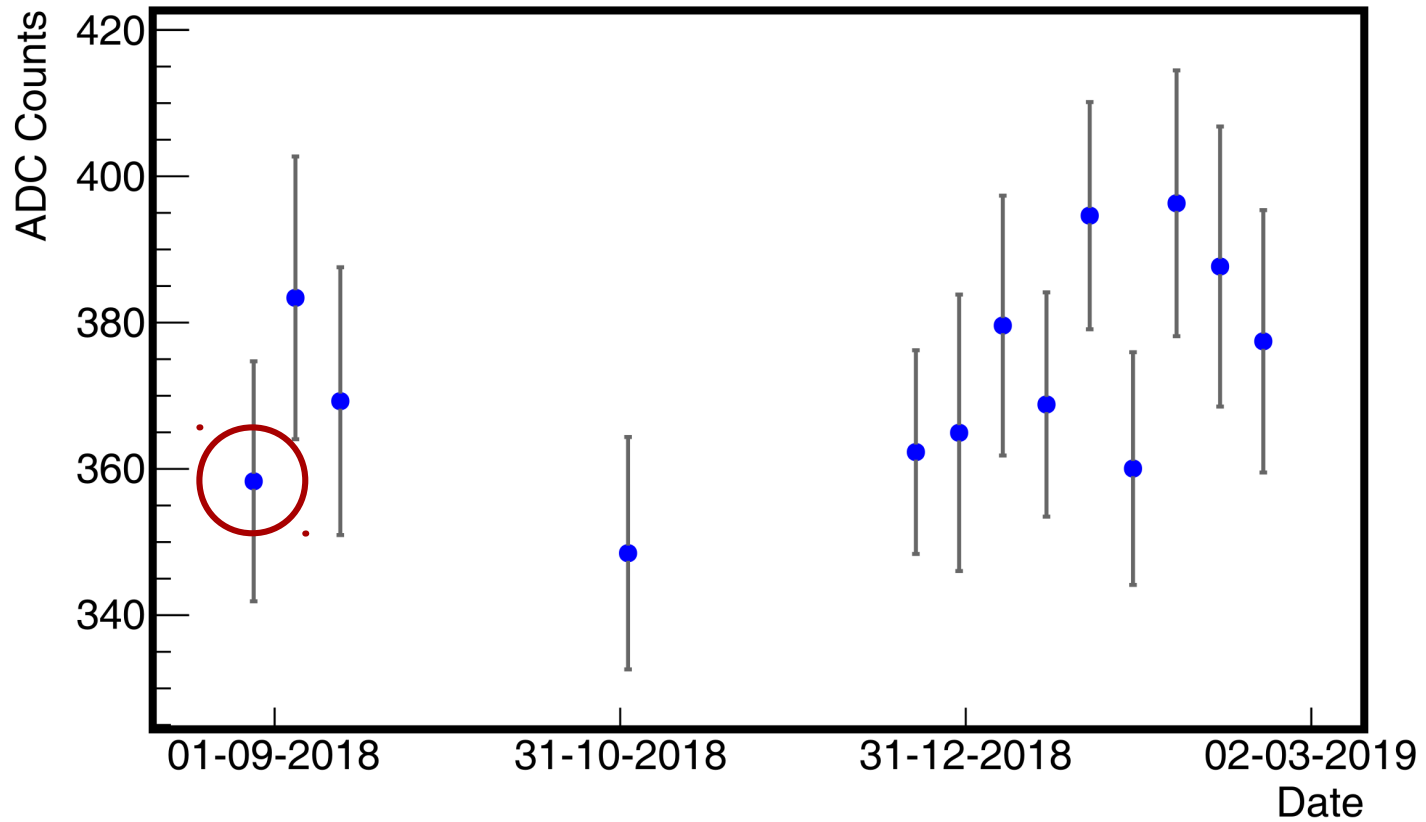
T1 muon mean: (358 ± 7) ADC Counts

Offline calibration with T3 events



T3 muon mean: (343 ± 4) ADC Counts

Long term monitoring and stability



Mean: 373
RMS: 14

**< 4% fluctuation
in this range.**

BKP

$$E_{\gamma, e^\pm} = E_{\text{ssd}}^{\gamma, e^\pm} + E_{\text{wcd}}^{\gamma, e^\pm}$$

$$m = \frac{E_{\text{ssd}}^{\gamma, e^\pm}}{E_{\text{ssd}}^{\gamma, e^\pm} + E_{\text{wcd}}^{\gamma, e^\pm}}$$

$$E_{\mu^\pm} = E_{\text{ssd}}^{\mu^\pm} + E_{\text{wcd}}^{\mu^\pm}$$

$$n = \frac{E_{\text{ssd}}^{\mu^\pm}}{E_{\text{ssd}}^{\mu^\pm} + E_{\text{wcd}}^{\mu^\pm}}$$

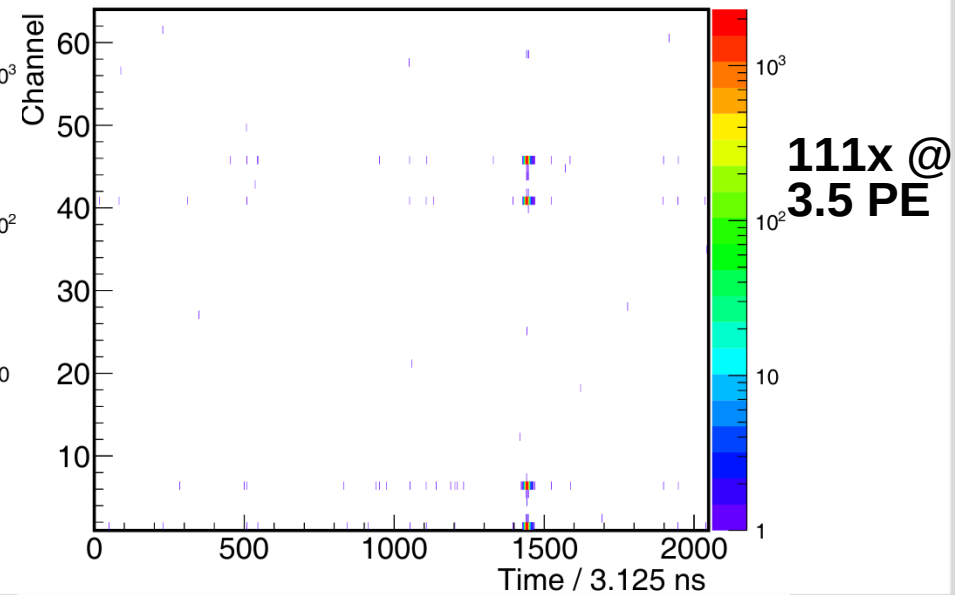
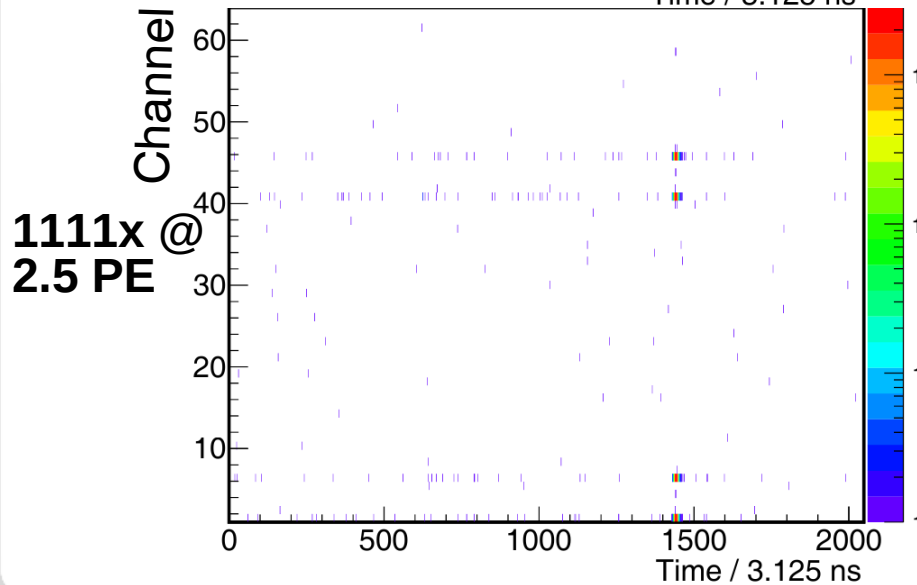
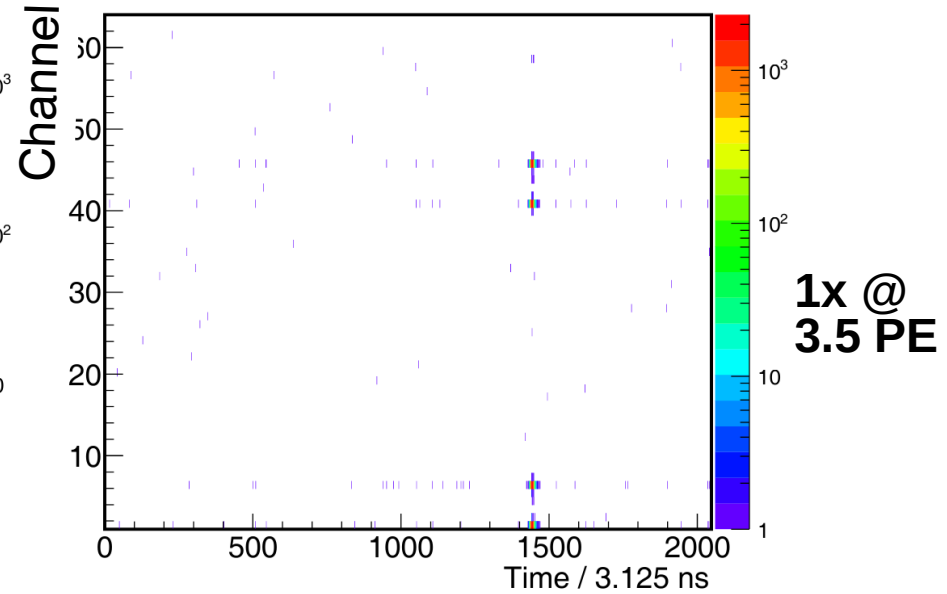
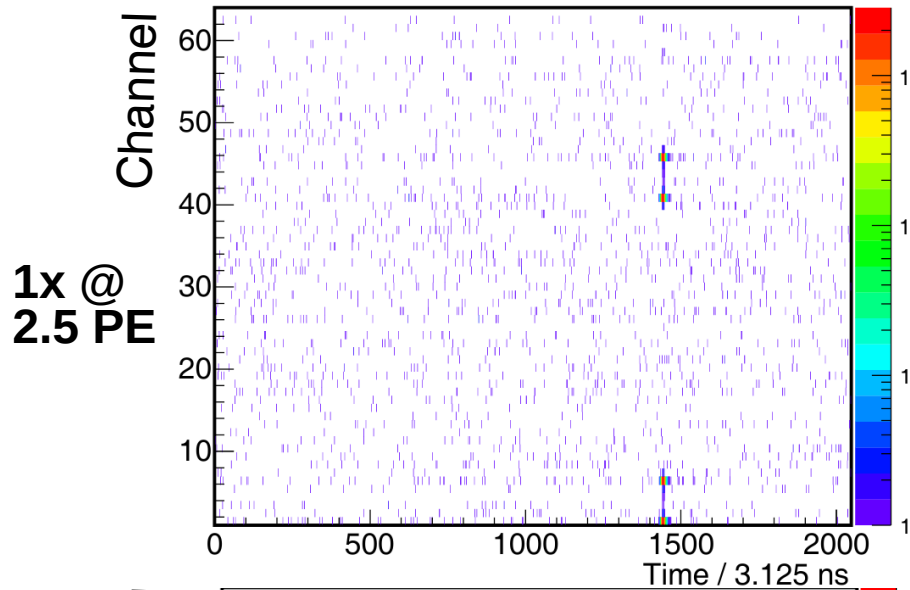
$$\begin{pmatrix} E_{\text{ssd}} \\ E_{\text{wcd}} \end{pmatrix} = \begin{pmatrix} m & n \\ 1 - m & 1 - n \end{pmatrix} \begin{pmatrix} E_{\gamma, e^\pm} \\ E_{\mu^\pm} \end{pmatrix}$$

$$E_{\text{wcd}}^{\gamma, e^\pm} = \frac{1 - m}{m - n} [(1 - n)E_{\text{ssd}} - nE_{\text{wcd}}]$$

$$E_{\text{wcd}}^{\mu^\pm} = \frac{1 - n}{m - n} [(m - 1)E_{\text{ssd}} + mE_{\text{wcd}}]$$

D. Schmidt, Ph.D.
Thesis

Counting strategy: patterns (1x, 111x, 1111x)



$$N^A_{EM,\max}(E_0) = AN^P_{EM,\max}(E_0/A) \approx N^P_{EM,\max}(E_0)$$

$$X^A_{\max}(E_0) = X^P_{\max}(E_0/A), \quad \text{and}$$

$$N^A_{\mu} = A \left(\frac{E_0/A}{E_{\text{dec}}} \right)^{\alpha} = A^{1-\alpha} N^P_{\mu}(E_0)$$